University of Padova

Department of Civil, Environmental and Architectural Engineering

Master Thesis in Environmental Engineering

Simulation of the Performance of Thermal Energy Storage Systems for the Cold Chain in Developing Countries

Supervisor
Prof. Simone Mancin
University of Padova

Co-supervisor
Prof. Marco Noro
University of Padova

Master Candidate
Nigar Gasimova

Student ID
2005917

Academic Year
2022-2023

Abstract

Approximately 10% of all electricity consumption worldwide is used for cooling, and this number is expected to increase rapidly as the world's population grows [1]. The increasing need for cooling in food storage facilities is directly related to the rising temperature trend worldwide. But one of the means of turning this temperature increase into an opportunity is solar cooling, which has many environmental advantages, such as lowering the need for the main grid and cutting down on greenhouse gas emissions.

This thesis provides a case study of a solar photovoltaic (PV) powered refrigerated container ($25m \times 40m \times 5m$) with integrated Thermal Energy Storage (TES) which gives a great opportunity to minimize the need for grid electricity while yet keeping perishable foods at constant temperature in Venice, Italy. TRNSYS software has been used to run a dynamic simulation of the case study system. The system consists of a container, vapour compression chiller, PV panel and TES. To calculate the cooling load of the container, the stratification of the walls, heat gains and the dimensions of the container are added to TRNBuild. After connecting the container, chiller, and PV to the weather data, and fixing the inlet and outlet temperatures of the chiller, the mass flow rate of the refrigerant was calculated and sent back to the system as input. To determine how much solar energy is needed to fulfil the electricity demand of the chiller, different PV areas are simulated. One of the main focal points of this thesis is how much electricity we save with different capacities of TES and areas of PV panels.

The results show that the total amount of electricity saved during the year varies considerably depending on the season. Minimum savings occur in winter because of the chiller's low power consumption and the TES's near-constant charging level, while in summer PV panels cannot fully cover the demand of the chiller even using with high capacities TES, so saved energy percentages are also lower in summer months. On the other hand, increasing TES size capacity and reducing PV areas can have a positive impact both economically and in terms of energy.

Acknowledgments

My thesis supervisor, Prof. Simone Mancin, was really helpful throughout the process, and I would like to thank him for his time and effort. Also, I would like to express my gratitude to Prof. Marco Noro for instructing me in the use of the TRNSYS simulation program. I am grateful for the support and encouragement I received from my lovely family and my wonderful partner while writing my thesis.

Nigar Gasimova
Padova, Italy
March 2023

Contents

Abstract **v**

List of figures **x**

List of tables **xiii**

Listing of acronyms **xv**

1 Introduction **1**
- 1.1 Research Background . . . 1
- 1.2 Energy Landscape in Veneto, Italy . . . 4
- 1.3 Contribution . . . 6
- 1.4 Outline . . . 7

2 Case Study **9**
- 2.1 Cold storage chamber model . . . 11
- 2.2 Location and Weather data description . . . 17
- 2.3 Chiller Model . . . 19
- 2.4 PV Model . . . 21
  - 2.4.1 Annual period . . . 22
  - 2.4.2 Winter month (January) . . . 24
  - 2.4.3 Summer month (July) . . . 27
  - 2.4.4 15th of January . . . 30
  - 2.4.5 15th of July . . . 32

3 Results **35**
- 3.1 PV area of $200m^2$ . . . 44
- 3.2 PV area of $300m^2$ . . . 47
- 3.3 PV area of $400m^2$ . . . 50
- 3.4 PV area of $600m^2$ . . . 52
- 3.5 Annual analysis . . . 55

4 Conclusion **59**

References **61**

Listing of figures

1.1 Solar Cooling Technologies [2] 2
1.2 Basic Vapor-Compression cooling cycle 4
1.3 Gross production of electricity from renewable sources (GWh), Veneto and Italy. (Veneto, 2019) 5
1.4 Gross production of electricity from renewable sources by type of source (GWh), Veneto. (Veneto, 2019) 6

2.1 Configuration of cold storage driven by PV system. 10
2.2 Schematic representation of the simulation approach used. 11
2.3 Model flow diagram in TRNSYS. 12
2.4 Sketch of container in TRNBuild. 13
2.5 Cooling Load and Air Temperature of the container. 16
2.6 Mean value of the monthly cooling load. 17
2.7 Daily ambient temperature in Venice. 18
2.8 Total incident radiation on roof and west, north walls of the container. 18
2.9 Total incident radiation on the south and east walls of the container. 19
2.10 Calculation of water mass flow rate in TRNSYS. 20
2.11 Water mass flow rate. 20
2.12 Chiller power. 21
2.13 Comparison between annual power of $400m^2$ PV and chiller. 22
2.14 Comparison between annual power of $300m^2$ PV and chiller. 23
2.15 Comparison between annual power of $200m^2$ PV and chiller. 24
2.16 Comparison between $15m^2$ PV and chiller powers in January. 25
2.17 Comparison between $20m^2$ PV and chiller powers in January. . . . 26
2.18 Comparison between $100m^2$ PV and chiller powers in January. . . . 27
2.19 Comparison between $400m^2$ PV and chiller powers in July. 28
2.20 Comparison between $490m^2$ PV and chiller powers in July. 29
2.21 Comparison between $500m^2$ PV and chiller powers in July. 30
2.22 Comparison between $1000m^2$ PV and chiller powers on 15th of January. 31
2.23 Comparison between $5000m^2$ PV and chiller powers on 15th of January. 32
2.24 Comparison between $480m^2$ PV and chiller powers on 15th of July. 33
2.25 Comparison between $500m^2$ PV and chiller powers on 15th of July. 34

3.1 Saved electricity percentages using only PV. 36
3.2 Saved electricity percentages using PV and 10 kWh TES. 37

3.3 Saved electricity percentages using PV and 20 kWh TES. 38
3.4 Saved electricity percentages using PV and 50 kWh TES. 39
3.5 Saved electricity percentages using PV and 100 kWh TES. 40
3.6 Saved electricity percentages using a different capacity of TES with $200m^2$ PV. 41
3.7 Saved electricity percentages using a different capacity of TES with $300m^2$ PV. 42
3.8 Saved electricity percentages using a different capacity of TES with $400m^2$ PV. 43
3.9 Saved electricity percentages using a different capacity of TES with $600m^2$ PV. 44
3.10 Level of TES with $200m^2$ PV in January. 45
3.11 Level of TES with $200m^2$ PV in April. 46
3.12 Level of TES with $200m^2$ PV in July. 46
3.13 Level of TES with $200m^2$ PV in October. 47
3.14 Level of TES with $300m^2$ PV in January. 48
3.15 Level of TES with $300m^2$ PV in April. 48
3.16 Level of TES with $300m^2$ PV in July. 49
3.17 Level of TES with $300m^2$ PV in October. 49
3.18 Level of TES with $400m^2$ PV in January. 50
3.19 Level of TES with $400m^2$ PV in April. 51
3.20 Level of TES with $400m^2$ PV in July. 51
3.21 Level of TES with $400m^2$ PV in October. 52
3.22 Level of TES with $600m^2$ PV in January. 53
3.23 Level of TES with $600m^2$ PV in April. 53
3.24 Level of TES with $600m^2$ PV in July. 54
3.25 Level of TES with $600m^2$ PV in October. 54
3.26 Annual saved energy (%) with $200m^2$ PV and different TES capacities. 55
3.27 Annual saved energy (%) with $300m^2$ PV and different TES capacities. 56
3.28 Annual saved energy (%) with $400m^2$ PV and different TES capacities. 56
3.29 Annual saved energy (%) with $600m^2$ PV and different TES capacities. 57
3.30 Annual saved energy (%) with different PV and TES. 58

Listing of tables

2.1 TRNSYS model's components 11
2.2 Properties of construction materials 14

Listing of acronyms

PV ..... Photovoltaic

Poly-Si ..... Polycrystalline Silicon

IT ..... Information Technology

TES ..... Thermal Energy Storage

CapEx ..... Capital Expenditure

OpEX ..... Operational Expenditure

TRNSYS .... Transient Systems Simulation Program

TMY ..... Typical Meteorological Year

EU ..... European Union

VFD ..... Variable Frequency Drive

HVAC ..... Heating, Ventilation and Air Conditioning

kWh ..... kiloWatt-hour

1 Introduction

1.1 Research Background

Increases in the rates of energy consumption have been shown to be a useful indication for the development of civilisation over the history of humankind. It seems that the quantity of energy utilized on a per capita basis is linked to both a country's level of industrialization and the quality of life. According to the conclusions of the studies, greenhouse gas emissions are anticipated to cause a median global warming of around $3.2°C$ by 2100 [3]. This is a result of the tremendous revolution in all human activity using fossil fuels. As a consequence, the earth is presently experiencing detrimental air pollution on a scale never previously witnessed in human history.

To mitigate these unintended consequences, it is essential that we significantly cut down on the hazardous emissions caused by the utilization of fossil fuels. Either boosting the efficiency of the system's energy conversion from fossil fuels or switching to green energy would accomplish this. Due to its endless availability and global distribution, solar energy stands out among these options as the most promising [4]. Also, unlike fossil fuels, solar energy can be easily collected and does not contribute to global warming or alter the Earth's surface.

The concept of solar-powered cold storage is a topic of tremendous interest due

to the numerous potential benefits and practical applications of solar energy today. Cold storage facilities, whether standalone structures or sections of a larger complex, use temperature control to ensure the quality of perishable foods within a certain temperature range which is crucial to extending and guaranteeing their shelf life; Since temperature variations may hasten the spoilage or compromise the integrity of many products, keeping them in the fridge is a must. Damage from excessive heat may spoil not just perishable food and medicine but also cosmetics, house furnishings, and fabrics, leading to economic damage. Cooling these perishables helps slow down their physical and chemical changes, protecting their purity and preventing biological degradation. Cold storage container aims to facilitate the distribution of perishable goods to consumers while minimizing spoilage and maximizing product viability. With solar cooling, the quantity of energy needed to refrigerate requirements is drastically reduced, leading to financial savings and environmental benefits through the utilization of renewable energy and the elimination of ozone-depleting substances.

Studies conducted on solar-powered cooling systems showed their viability in comparison to more traditional methods when they were well-designed. Based on whether the solar radiation is transformed into heat (solar collectors) or electric power (photovoltaic panels), solar cooling technologies can be divided into thermal and electrically powered systems [2] (figure 1.1). Their operational temperature ranges and underlying operating principles also allow for further categorization. These innovations can provide refrigeration and freezing choices in addition to air conditioning, food storage, and pharmaceutical preservation.

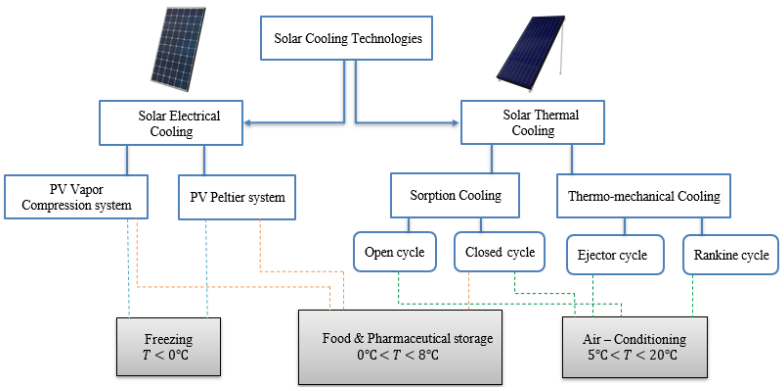

Figure 1.1: Solar Cooling Technologies [2]

One of the most important considerations for the widespread use of solar cooling technology is its cost-effectiveness. The financial viability of solar cooling systems has been examined by numerous experts [5]. According to studies in 2008, solar electric cooling systems had a higher equipment cost than solar thermal cooling systems [6]. Yet, a different study shows that by 2030, the equipment cost of solar PV cooling systems will have decreased significantly, while the cost of solar thermal cooling systems had decreased only slightly [7]. Economically, solar PV cooling systems have been shown to outperform solar thermal conversion cooling systems in a number of recent studies. Based on data from Abu Dhabi, researchers analyzed 25 diverse solar cooling systems, each with their own unique design, and the findings revealed that the long-term economic performance of solar absorption cooling systems with single-effect absorption chillers and flat plate collectors was inferior to that of solar PV cooling systems with vapour compression chillers and poly-Si photovoltaic cells [8]. The financial viability of solar-powered electricity and thermal cooling systems was also investigated in two separate studies that factored in weather conditions (in Spain and the Netherlands) [9]. Both studies demonstrated that the PV cell and water-cooling compression chiller combination was the most cost-effective cooling system, regardless of environment, and that the total cost of all PV cooling systems was less than that of solar thermal systems.

Putting aside the financial considerations discussed in the aforementioned studies, there are numerous more reasons why PV panel cooling systems have become increasingly popular in recent years [10]:

- Basic design: a PV system's connection is typically made up of electrical cable, which makes for a quick and painless installation. Also, the system's key parts are all well-established and readily accessible, making it a simple construction.
- Controlling and integrating the PV system with IT is simple, allowing for optimum control and remote monitoring to be performed with little effort. A vapour compression refrigeration system's ability to rapidly adjust its cooling output to meet fluctuating cooling demands is a key advantage.
- Green energy and less pollution thanks to the system's ability to make full use of locally generated energy while reducing its reliance on the grid. This function will be especially useful during the summer months when high temperatures and increased demand for electricity put additional pressure on the power grid.

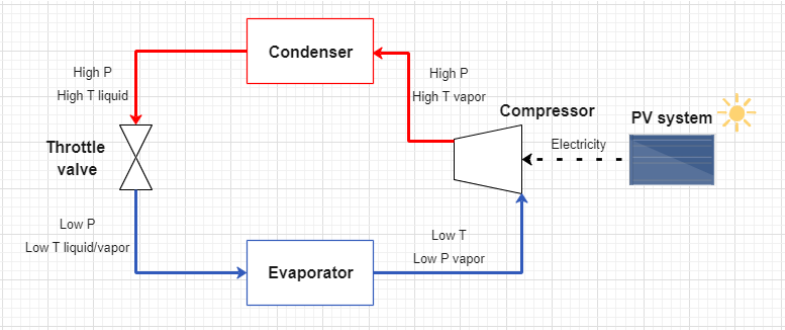

Figure 1.2: Basic Vapor-Compression cooling cycle

Conventional vapour-compression chillers powered by electricity from PV panels are the most widespread type of refrigeration. These systems are examples of vapour cycles, in which the refrigerant (working fluid) changes phase at least once during operation. Vapour compression refrigeration relies on the refrigerant evaporating at low temperatures to provide cooling. The cooling capacity of vapour compression systems ranges from a few watts to a few megawatts, making them suitable for almost any application [11].

Since weather data might cause fluctuations in PV electricity generation, there are occasions when PV power production does not coincide with chiller demand. Thus, thermal energy storage is necessary to buffer the fluctuations in the supply and demand for electricity. The term "thermal energy storage" refers to a technique that allows for the temporary storage of thermal energy by either heating or cooling a storage medium for the purpose of later usage in heating and cooling systems or in the production of electricity. Using TES in a power system has several benefits, including better operational flexibility, lower CapEx and OpEx, and less environmental impact [12].

1.2 Energy Landscape in Veneto, Italy

Venice, the capital of the Veneto region in northeastern Italy, is located on an island in the crescent-shaped Venice Lagoon, which runs approximately 51 kilometres from the marshes of Jesolo in the north to the areas beyond Chioggia in the south [13]. The current estimate for the year 2023 has Venice's population at 258,051 [14].

Coal, oil and natural gas were the main sources of Venice's energy sector [15]. As the energy sector accounts for 78% of EU greenhouse gas emissions and more

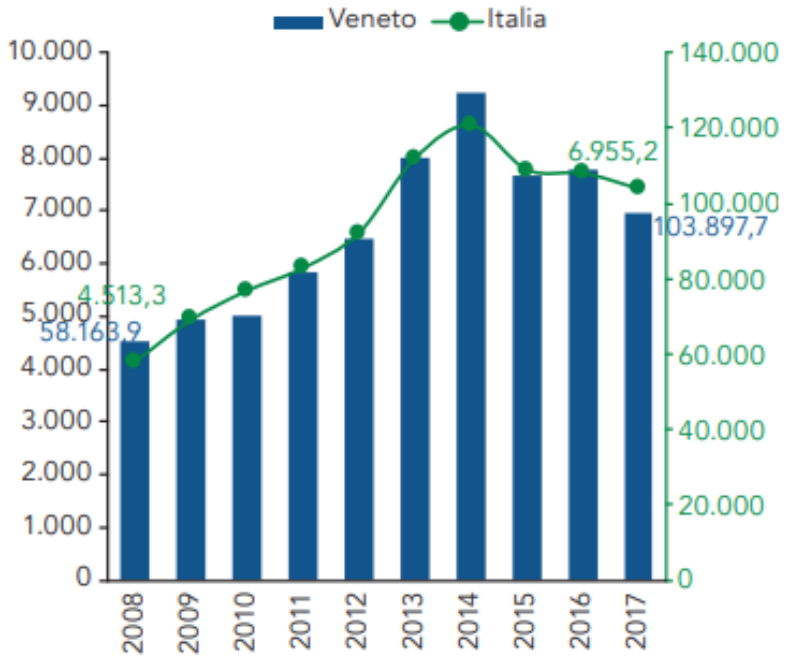

Figure 1.3: Gross production of electricity from renewable sources (GWh), Veneto and Italy. (Veneto, 2019)

than 81% for Italy, it must play a pivotal role in any effort to reduce pollution. The European Union has established to new goals for decreasing energy use and expanding renewables, including increasing renewable energy production to 27% by 2030 and improving energy efficiency by the same amount [16].

Solar energy now makes up a 5^{th} of the renewable energy sector, although only provides enough energy for between 7% and 8% of Italy's total energy demand. Photovoltaic panels are the most common kind of solar energy used in Italy. There is also solar thermal generating, although it does not account for a substantial fraction (<1%) of the country's total solar energy production [17].

The percentage of electricity generated in Italy and the Veneto region from renewable sources increased from 18.2% to 35.1% and from 26.1% to 42.3%, respectively, throughout the 9 years starting in 2008. Veneto's high percentages come from the region's growing solar and bioenergy industries, although overall production has been steadily declining. When comparing 2008 and 2017, the number of solar installations jumps from 3000 to 106000. The PV industry in Veneto surpassed 1,850,000 kW in installed capacity by the end of 2017. The decline in this last figure since 2011 points to a structural shift in the industry, whereby more installations

are being built at lower scales [16].

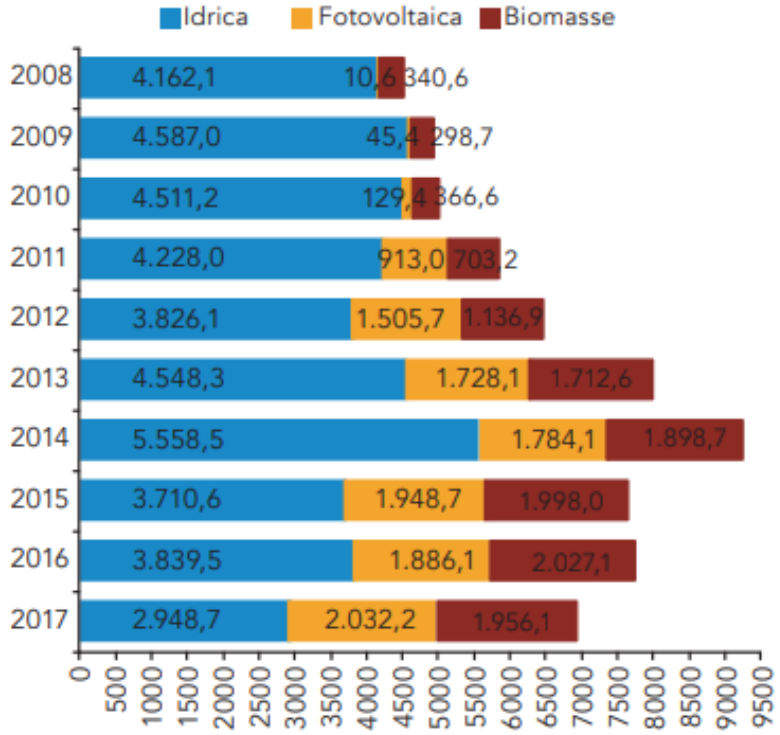

Figure 1.4: Gross production of electricity from renewable sources by type of source (GWh), Veneto. (Veneto, 2019)

1.3 Contribution

The purpose of this thesis is to know more about the efficiency and effectiveness of a solar photovoltaic-powered cold chamber and thermal energy storage system in the humid subtropical climate of Venice, Italy. The chamber is cooled by solar PV panels and kept at 5 degrees Celsius, an optimal temperature for keeping food. In designing the structure in TRNSYS simulation software, we also calculated the annual cooling load of the building in order to incorporate a vapour compression chiller and photovoltaic panels. On the one hand, we optimized the adequate area required for the PV panel to meet the electricity for the chiller by comparing the energy required to cool the building with energy from the chiller on the other. At last, significant results on the efficiency and scale of TES systems are presented,

along with a brief overview of thermal energy storage. The following targets will be pursued by means of this study:

- Creating a building model with the help of the TRNBuild tool in the TRNSYS simulation program and being sure to identify the design, orientation, material, heat gains and other operating characteristics of the structure.
- Running experiments to assess the chamber's energy efficiency and the cooling load needed to keep the temperature at $5°C$.
- To ensure that the energy needs of the vapour compression chiller for the container are met, it is necessary to size and simulate a solar PV system from the energy performance point of view.
- Excel will be used to calculate the electricity saved while taking into account four different PV areas and capacity of TES.
- Compile data from TRNSYS simulation and Excel, then provide conclusions.

1.4 Outline

This thesis is structured as follows. In Chapter 2, we discuss our research methods, providing some context for our study and describing the sites where it was conducted. Provides an overview of the TRNSYS software, system sizing and other core components of the system. Technical assessments of the solar PV system used to power the refrigeration system and also Excel calculations for determining TES volume are presented and discussed in Chapter 3. The results from the simulation and conclusion are outlined in Chapter 4.

2

Case Study

Figure 2.1 shows the basic layout of the cold storage system. The main components of this system are photovoltaic panels, a vapour compression chiller, a thermal energy storage device, and cold storage container. Fig 2.1 depicts the PV system's ability to directly power the system through the conversion of solar energy into electrical energy. Clouds and dust in the air hinder and disperse the sun's rays, which causes the output power of the PV arrays to vary in the directly driven system and, in turn, affects the consistency and efficiency of the load's running. To make sure the refrigerator could run adaptively at the time of maximal power production from the PV systems, the system's inverter and controller were combined into a single machine equipped with maximum power point tracking and frequency control technology. To power the chiller, the inverter transformed the direct current generated by the PV panels into an alternating current [18]. A variable frequency drive chiller, comprised of a VFD compressor, condenser, throttling valve, and evaporator, was used to handle the PV systems' varying output. The refrigeration cycle included the compression of saturated water vapour to produce high-pressure, high-temperature water vapour. Following that, water vapour was sent into the condenser, causing the vapour refrigerant to condense into water. As a result, the pressure and temperature of the water used as a refrigerant were lowered by throttling it. In the next phase, heat is absorbed during the vaporization process, quickly chilling the refrigerator's coils. When solar energy is insufficient to operate

the chiller, the energy stored in the thermal energy storage system may be put to use.

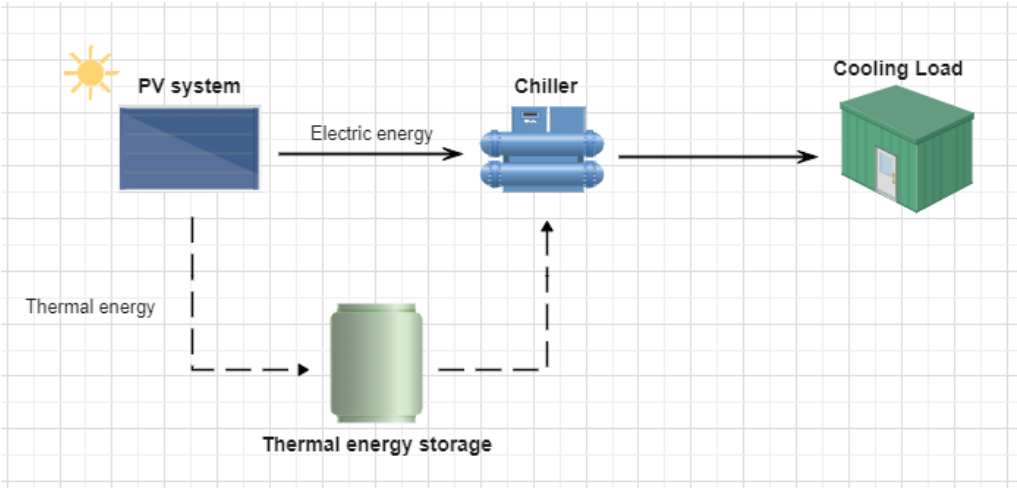

Figure 2.1: Configuration of cold storage driven by PV system.

A case study is conducted to explore the connections between TES and a PV cooling system for a cold chamber. TRNSYS (version 17), a transient simulation tool created by the University of Wisconsin-Solar Madison's Energy Laboratory, was used to model the case study. It has found widespread use in the simulation of solar heating and cooling systems [19]. The TRNSYS library contains functions that implement mathematical models of several components. As a result, TRNSYS may build a model of a system with any number of connections between its constituent parts. As soon as all parts of the system have been identified, a process flow diagram can be drawn up, with each part shown by a box that takes in some constant parameters and time-dependent inputs and gives out some time-dependent outputs. It is possible to feed an output back into the same system as an input. Using the flowchart in figure 2.2, we can illustrate the simulation approach used in this study. TRNSYS models were created, and then the system's parameters were calculated for the various experiments. The results of the simulations were examined thereafter. Table 2.1 provides a summary of the TRNSYS model's components.

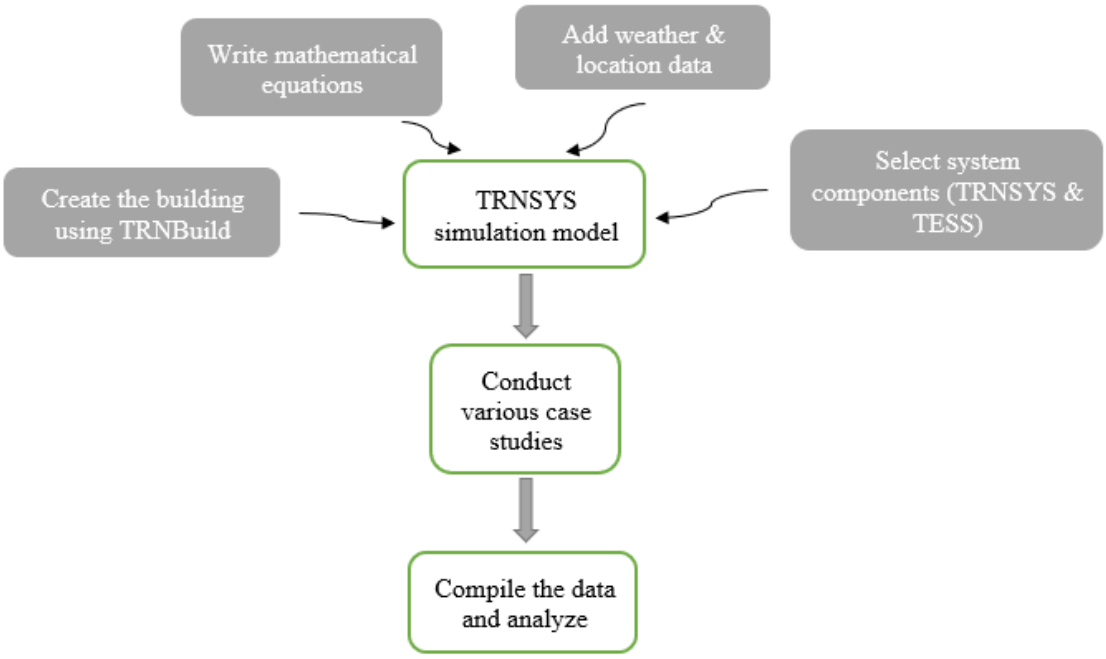

Figure 2.2: Schematic representation of the simulation approach used.

Table 2.1: TRNSYS model's components

Component table	Types	Comment
PV panel	Type 94a	Standard TRNSYS Ëlectrical" librar
Building	Type 56	Using TRNBUILD and linked to TRNSYS through type 56
Weather data	Type 15-6	Standard TRNSYS "Weather data Reading and Processing" library
Vapor compression chiller	Type 655	HVAC library (TESS)

2.1 Cold storage chamber model

The initial stage in modelling the case study was to use the visual building interface (TRNBuild) of TRNSYS 17 to create a building model for a refrigerated area with

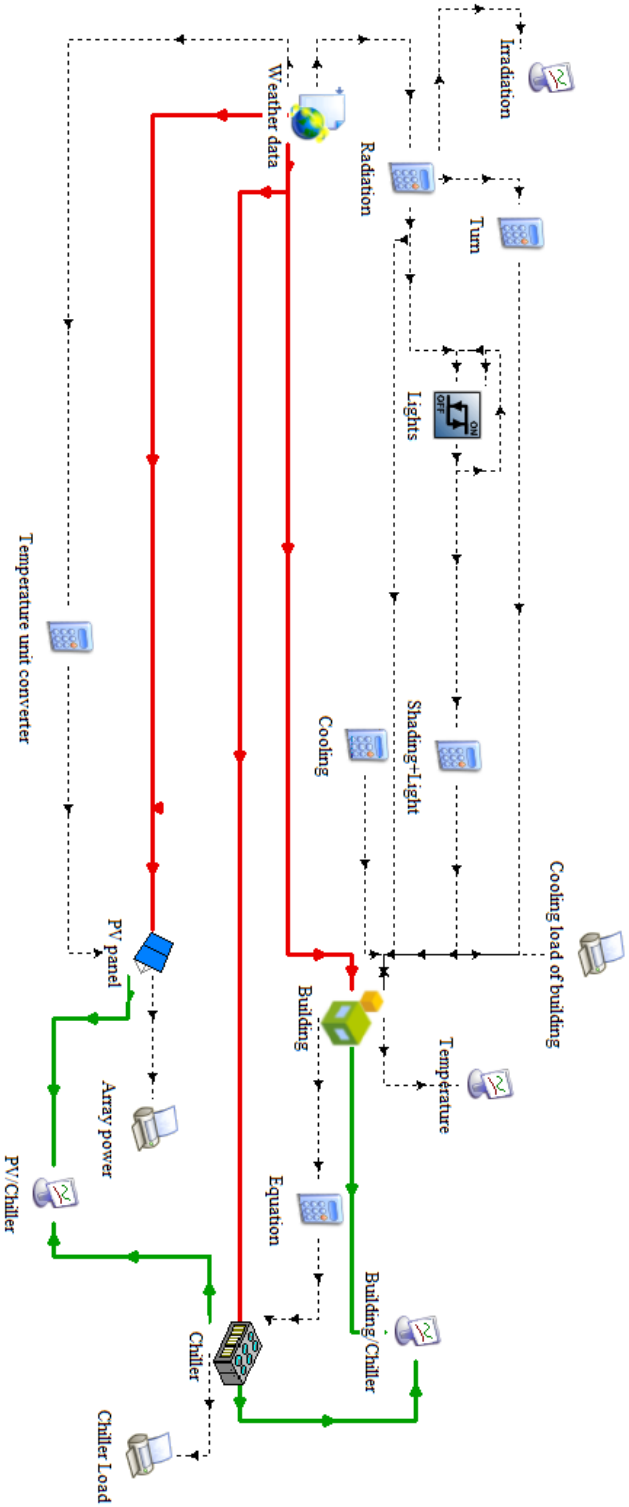

Figure 2.3: Model flow diagram in TRNSYS.

dimensions of $25m \times 40m \times 5m (5000m^3)$ in order to determine daily cooling load. When modelling TRNBuild and getting more realistic results from simulations, it is important to keep track of data on thermal zones, construction and occupancy. The model only has one thermal zone and no windows in order to restrict heat gain from outside. Warehouse food is brought into and taken out of the facility via a single, $4m \times 4m$ main entry door. A daily opening time of one hour (from 11:00 to 12:00) was taken into account. A sketch of the structure is shown in figure 2.4:

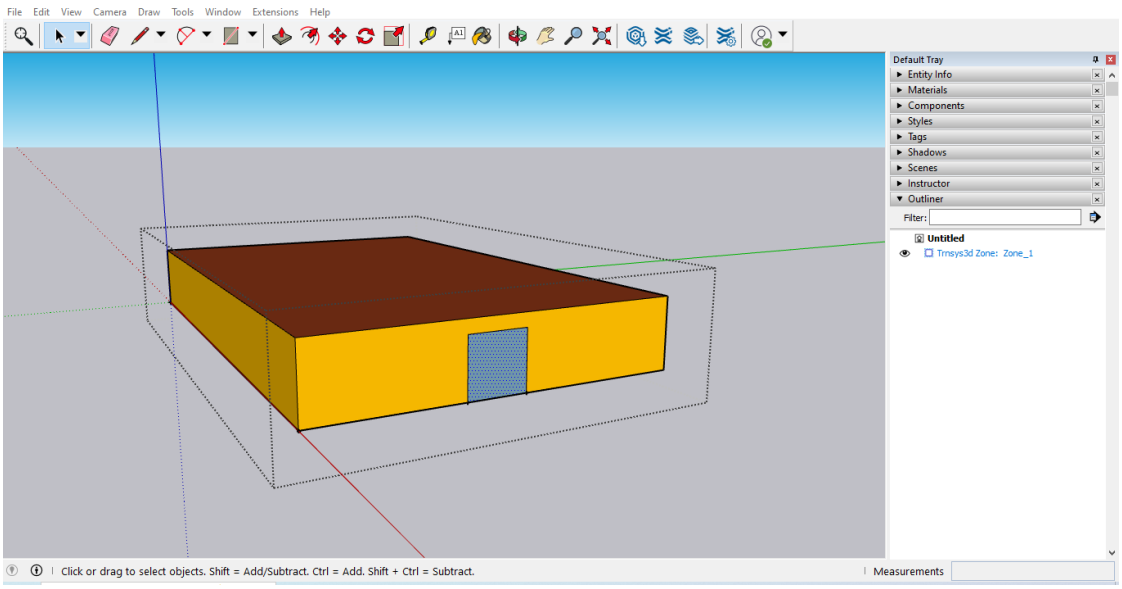

Figure 2.4: Sketch of container in TRNBuild.

The walls and roof are insulated with an 80 mm thick polyurethane foam, with a thermal conductivity of 0.0792 $\frac{kJ}{h*m*K}$ and a heat transfer coefficient of 1.453 $\frac{kJ}{K*kg}$ as it is shown in table 2.2:

Table 2.2: Properties of construction materials

Walls, Roof	**Thickness** (m)	**Conductivity** $(\frac{kJ}{h*m*K})$	**Capacity** $(\frac{kJ}{kg*K})$	**Density** $(\frac{kg}{m^3})$
Metal	0.001	475.2	0.935	2700
Polyurethane	0.08	0.0792	1.453	36
Pavement				
Concrete	0.2	3.1	0.8	2400

This cold storage container maintains a temperature of $5°C$ for the purpose of storing perishables. It is located in the northern hemisphere and both the cooling load and the chamber's energy balance are calculated by factoring in both external and internal heat gains. In order to keep the chamber at a given temperature, the amount of heat to be extracted from the chamber, in other words, cooling load is calculated by the following equation:

$$Q_{cooling} = Q_{product} + Q_{internal} + Q_{lights} + Q_{infiltration}$$

- $Q_{product}$ – New products entering the container generate heat, which is accounted for by this load. The sensible heat load is all that has to be considered if we're merely going to be cooling the products. When a product undergoes a phase transition, such as when it is frozen, latent heat must be taken into consideration. Product load is normally between 55% and 75% of the total cooling load. It is calculated as follows [20]:

$$Q_{product} = Q_{load} + Q_{respiration}$$

$$Q_{load} = C_p * m * (T_{in} - T_{out}) + m * Q_{res}(\frac{kWh}{day})$$

, where

  - C_p - specific heat capacity $(\frac{J}{kg*K})$
  - m - mass of products (kg)
  - T_{in} - initial temperature of product $°C$

  - T_{out} - temperature of product in cold storage $^{\circ}C$
  - Q_{res} - heat of respiration $(\frac{kJ}{kg})$

- $Q_{internal}$ – 10-20% of total cooling load is caused by internal loads. This is the temperature rise caused by the presence of workers and machinery such as forklift trucks, pallet jacks etc. in a refrigerated area. To do this, we must consider the tools the employees will require, the amount of heat they and the devices generate, and the length of time each day that these activities will take place [20].

$$Q_{internal} = t * Q_{people,equipment} * n_{people,equipment}(\frac{kWh}{day})$$

, where

  - t - duration of working hours (hr)
  - $Q_{people,equipment}$ - heat gain per people or equipment (W)
  - $n_{people,equipment}$ - number of people or equipment

- Q_{lights} – Lights that are activated only when the door is opened generate heat, often between 1% and 5% of the total load [20].

$$Q_{lights} = t * Q_{lamps} * n_{lamps}(\frac{kWh}{day})$$

, where

  - t - how much time lamps are on (hr)
  - Q_{lamps} - heat gain per lamp (W)
  - n_{lamps} - number of lamps

- $Q_{infiltration}$ – Another factor that must be considered is infiltration, increasing the cooling load by 1-10%, which happens whenever a door is opened and causes a transfer of heat into the area through the air. Infiltration airflow was set to a rate of 0.2 air changes per hour. Ventilation is a second factor

to think about. A ventilation fan should be installed in the storage area in order to remove excess moisture [20].

$$Q_{infiltration} = (T_{out} - T_{in}) * V_{storage} * n_{change} * Qm^3(\frac{kWh}{day})$$

, where

- $V_{storage}$ - volume of container (m^3)
- n_{change} - change in daily volume
- Q_{m^3} - heat gain per m^3 (W)

Using a time step of 1 hour and a dynamic simulation running all year (8760 hrs), the cooling demand was calculated to maintain an interior temperature of $5°C$. Figure 2.5 depicts the room temperature and cooling load and at 5532^{nd} hour of simulation time, the building cooling demand was at its highest $(72.6kW)$ (corresponding to 17th of August).

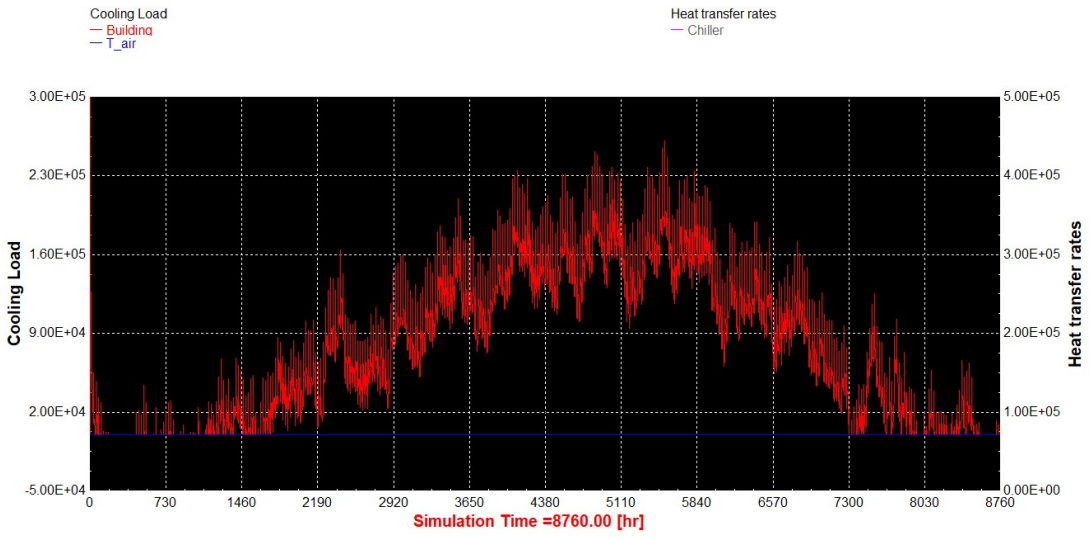

Figure 2.5: Cooling Load and Air Temperature of the container.

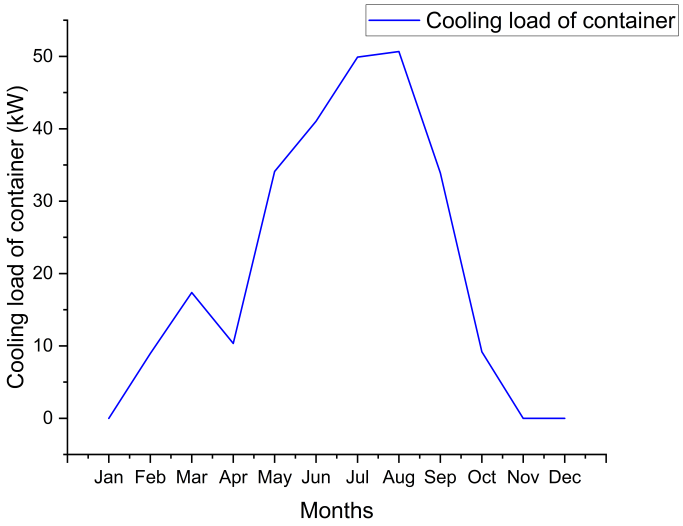

Figure 2.6: Mean value of the monthly cooling load.

2.2 Location and Weather data description

The efficiency of the container's energy model and PV system is significantly affected by the weather forecast. Each hour's value of weather information was averaged across 10 years, or one typical meteorological year (TM2). Daily data in one-hour intervals will be utilized for the simulation. Figures 2.7, 2.8, 2.9 show the daily dry-bulb ambient temperature and the hourly radiation on the surfaces of containers based on data from Meteonorm.

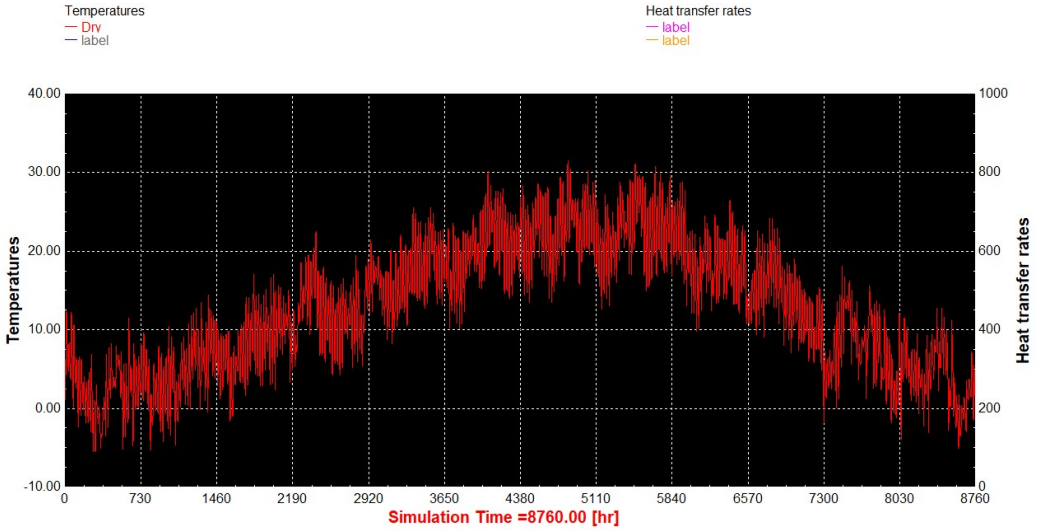

Figure 2.7: Daily ambient temperature in Venice.

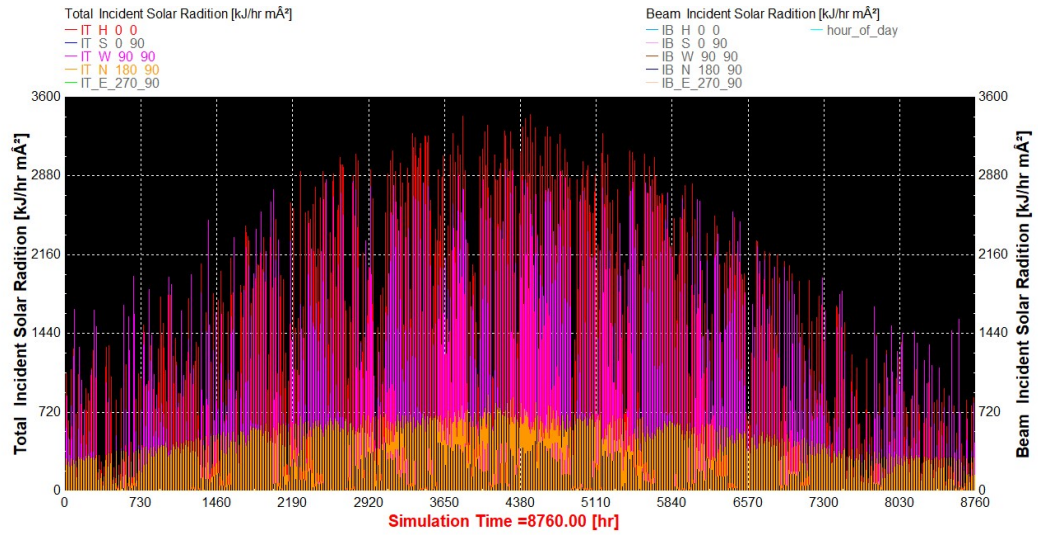

Figure 2.8: Total incident radiation on roof and west, north walls of the container.

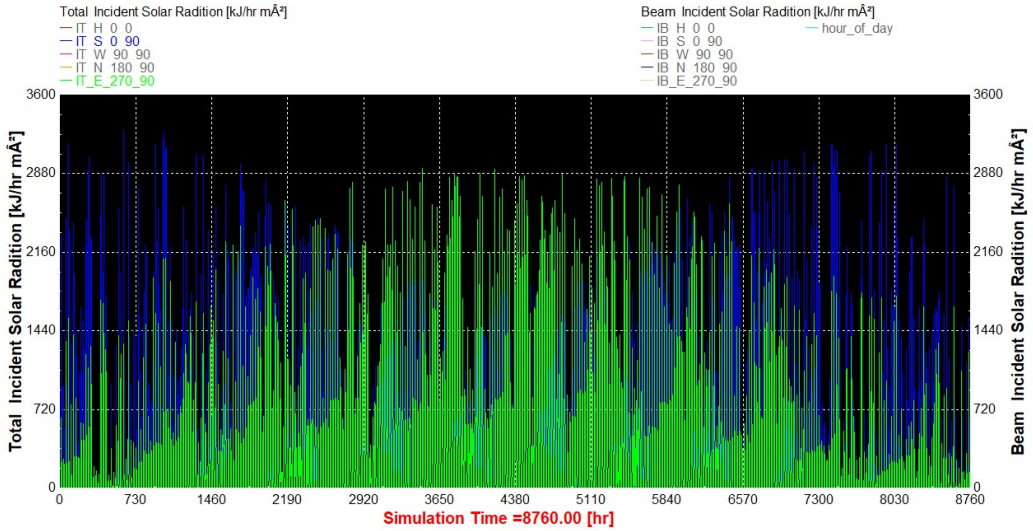

Figure 2.9: Total incident radiation on the south and east walls of the container.

2.3 Chiller Model

The container's inside temperature relies mainly on the performance of the chiller system. We used the "Equation" function of Trnsys to calculate the variable mass flowrate of water as the refrigerant and send it back as an input variable to the chiller, all while fixing the inlet and outlet temperatures of the chiller to 4 and 2, respectively to maintain a temperature of 5 within the container.

After that, we calculated how much power the chiller would need to constantly operate under the container's cooling load. The following graph shows the annual hourly power consumption required for the chiller, based on the accurate setup of chiller parameters and inputs. Based on the data, it is clear that the months of July and August have the highest average power consumption or electrical demand, at 8.4 kW and 8.6 kW, respectively.

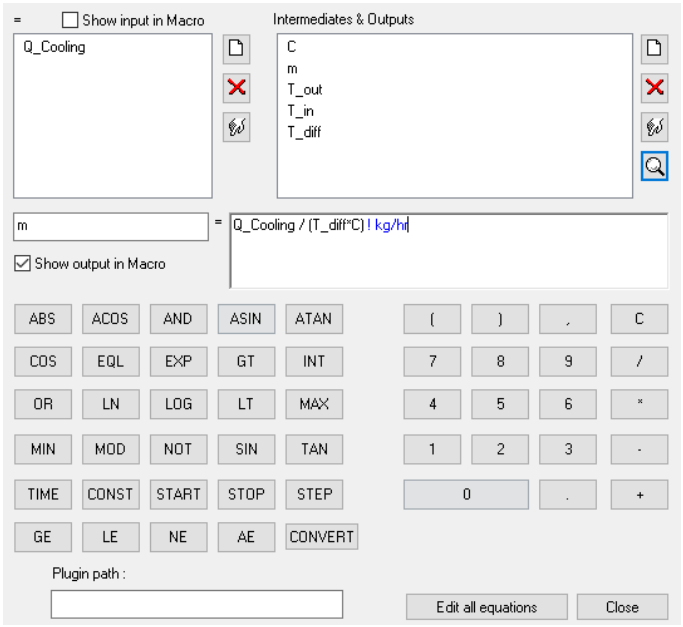

Figure 2.10: Calculation of water mass flow rate in TRNSYS.

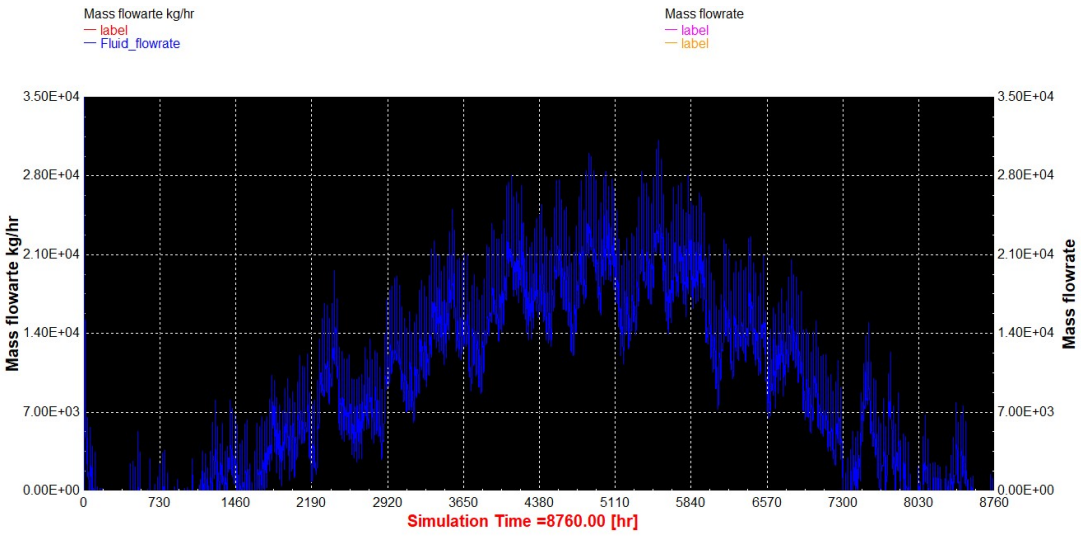

Figure 2.11: Water mass flow rate.

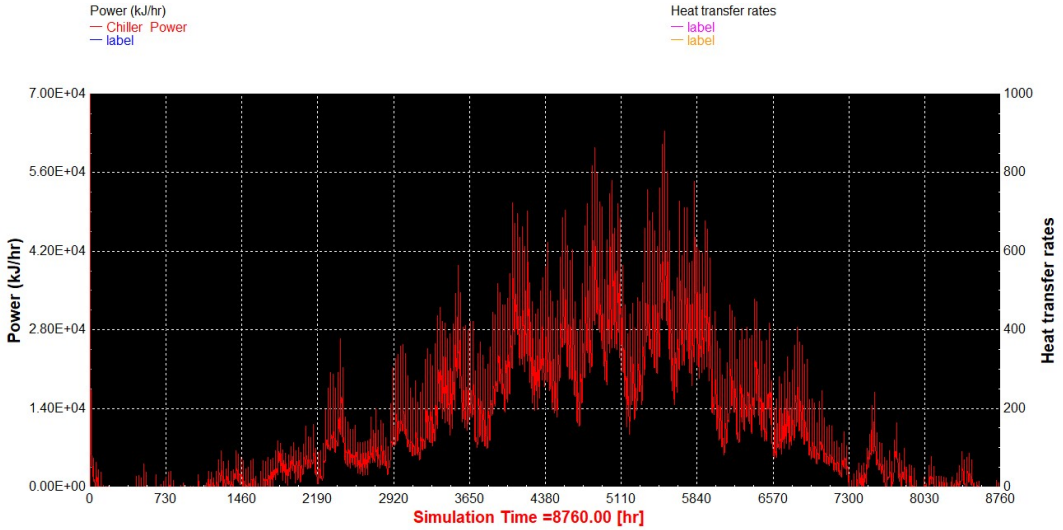

Figure 2.12: Chiller power.

2.4 PV Model

Electricity derived from solar photovoltaic panels as a source of power for the chiller is one of the primary objectives of this project. In order to properly size the PV system, it was necessary to determine the annual energy consumption of the chiller as part of the simulation and modelling phase of the study. First of all, the "Type 94-a/crystalline module" was selected as the PV panel in Trnsys, and while the ambient temperature, beam/diffuse radiation, and total incident radiation came from the "Type 15-6/weather data", other parameters were fixed as is common in the program, based on the catalogue data of the relevant manufacturers. The array slope is set at 30, and the PV panel has been configured to have 72 cells $(2.1m \times 1.1m)$ since this size is typical for larger roof areas or solar farms [21]. After changing the size of the PV modules' area, the resulting array power is compared to the amount of power required by the chiller in 5 different scenarios and the optimum area is decided for a given time period. To get an ideal area, the deficit between the annual sum of PV and chiller power should be roughly close to zero or more than zero, and the surplus energy can be stored in TES.

2.4.1 Annual period

Initially, the PV system and chiller were evaluated within one year. PV module areas are selected as $400m^2$, $300m^2$, and $200m^2$ using the trial and error method. Annual graphs for various PV areas show that the value of $(P_{PV} - P_{Chiller})$ is lowest (13.86 kW) for a $305m^2$ area, even without the use of TES.

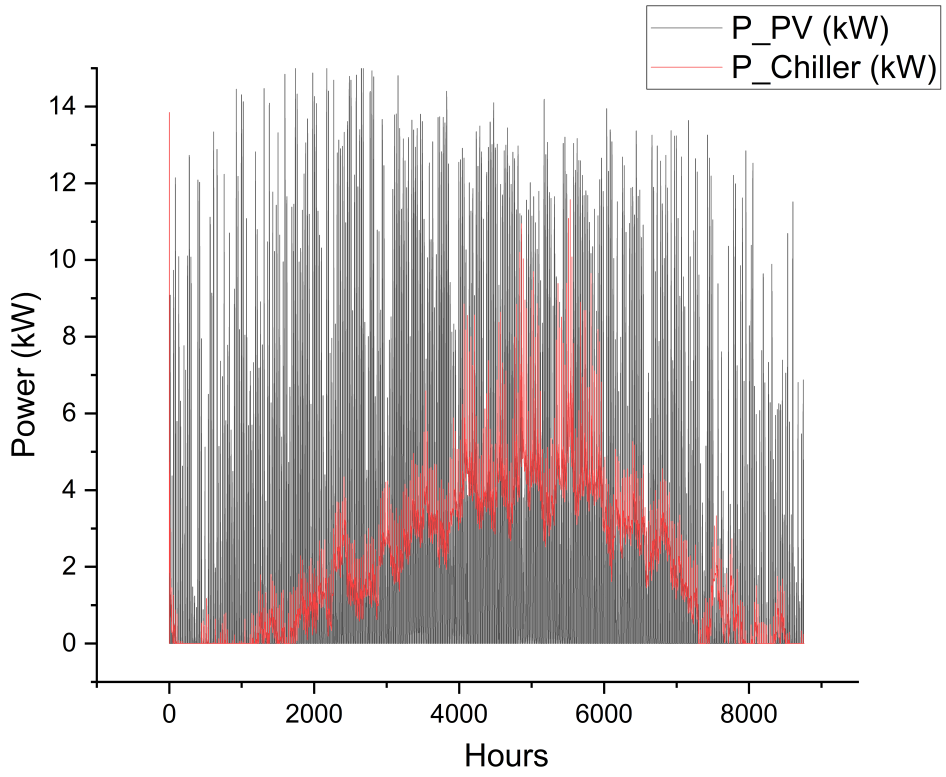

Figure 2.13: Comparison between annual power of $400m^2$ PV and chiller.

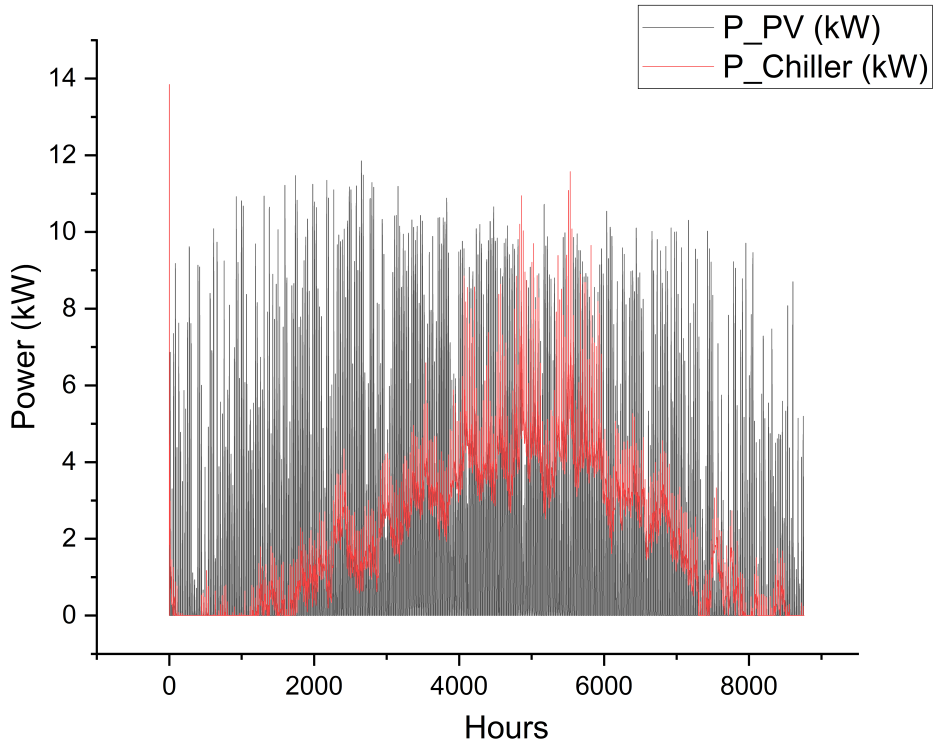

Figure 2.14: Comparison between annual power of $300m^2$ PV and chiller.

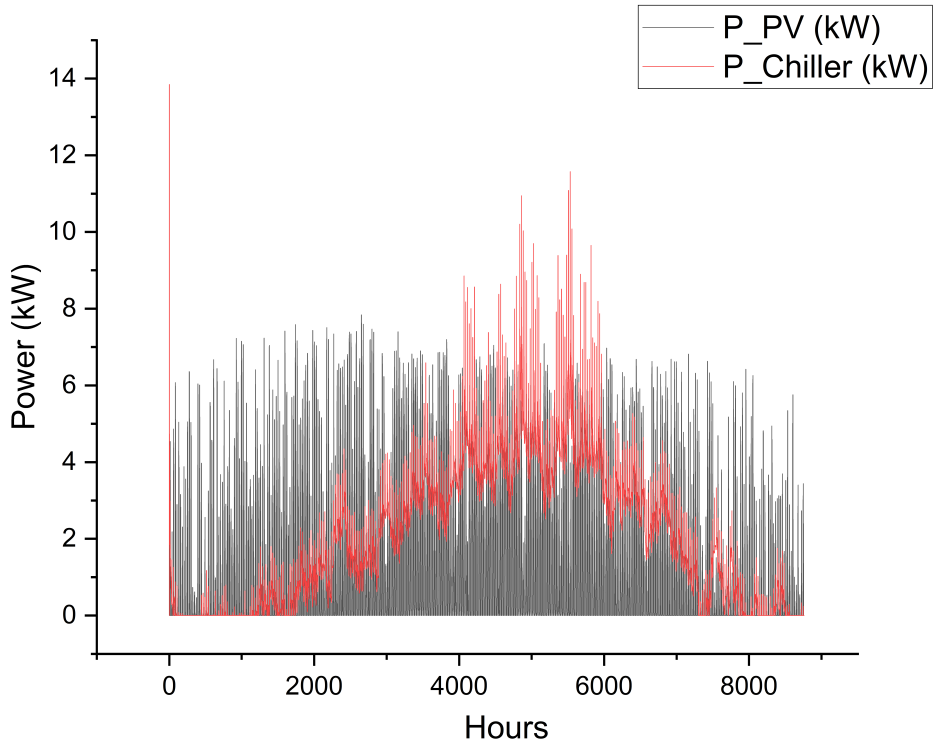

Figure 2.15: Comparison between annual power of $200m^2$ PV and chiller.

2.4.2 Winter month (January)

In the second case, only one winter month was considered. For January, $15m^2$, $20m^2$, and $100m^2$ areas of PV were checked. According to the figures, the minimum value of $(P_{PV} - P_{Chiller})$ is 23.5 kW at a surface area of $20m^2$. Because of the lower temperatures throughout the winter, a chiller doesn't need to use as much energy to reduce the refrigerant's temperature.

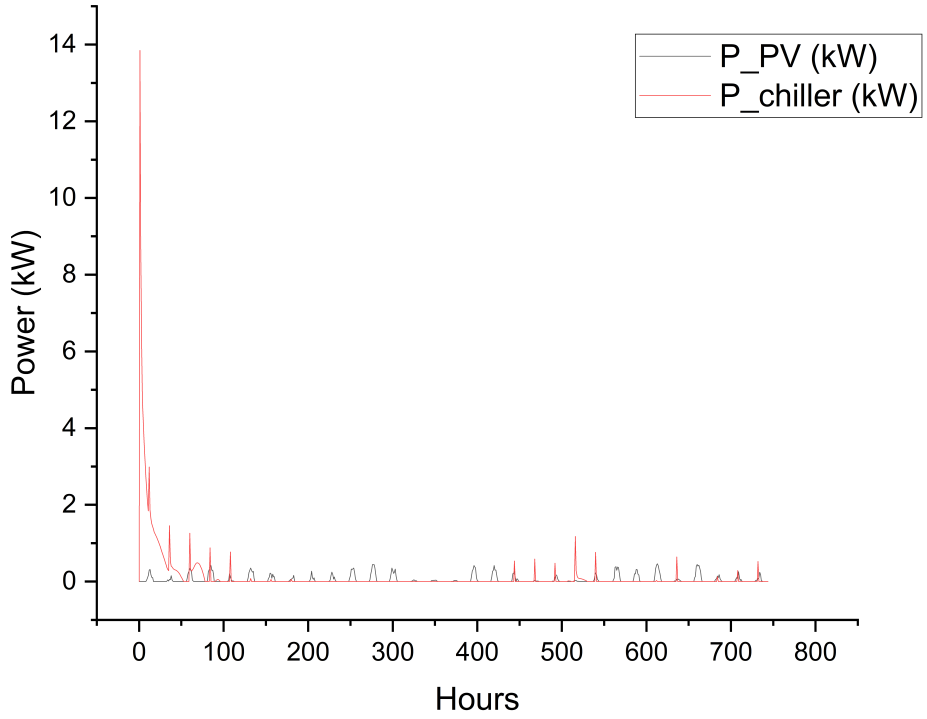

Figure 2.16: Comparison between $15m^2$ PV and chiller powers in January.

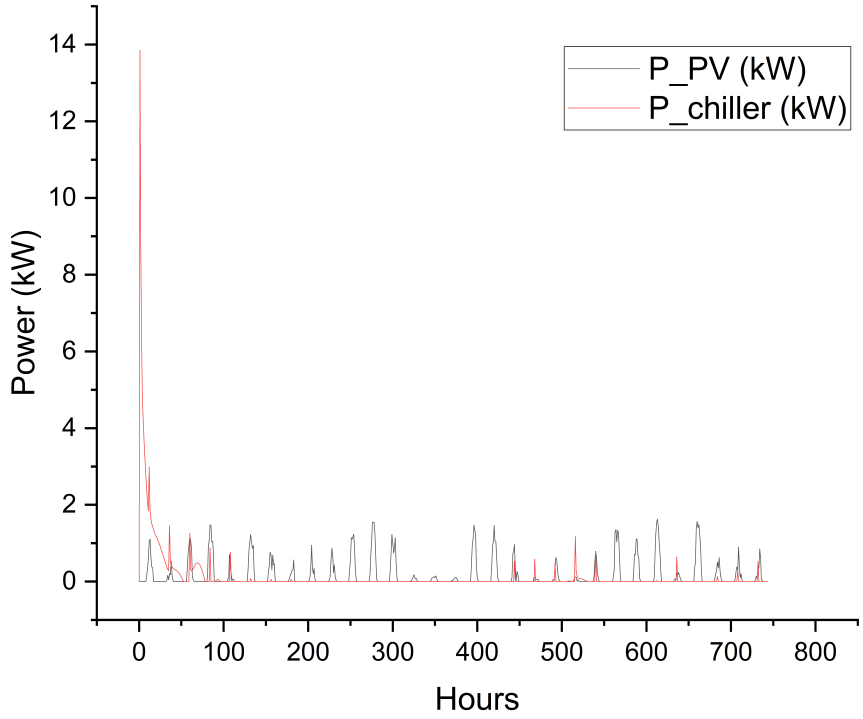

Figure 2.17: Comparison between $20m^2$ PV and chiller powers in January.

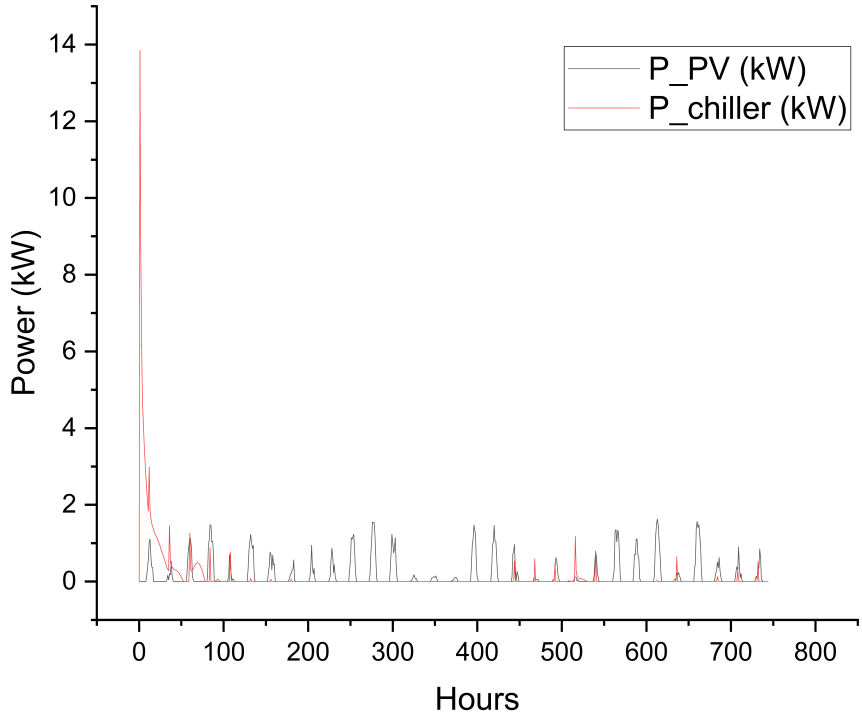

Figure 2.18: Comparison between $100 m^2$ PV and chiller powers in January.

2.4.3 Summer month (July)

In another case, the PV power and the power required to operate the chiller were checked for one of the summer months. The $400 m^2$, $490 m^2$, and $500 m^2$ PV plots have all been checked for the month of July. The minimal value of $(P_{PV} - P_{Chiller})$ is 47.6 kW at a surface area of $490 m^2$, as shown in figure 2.20. The reason why the area is large is that the chiller needs more electricity in summer and a large PV area is needed to cover this amount.

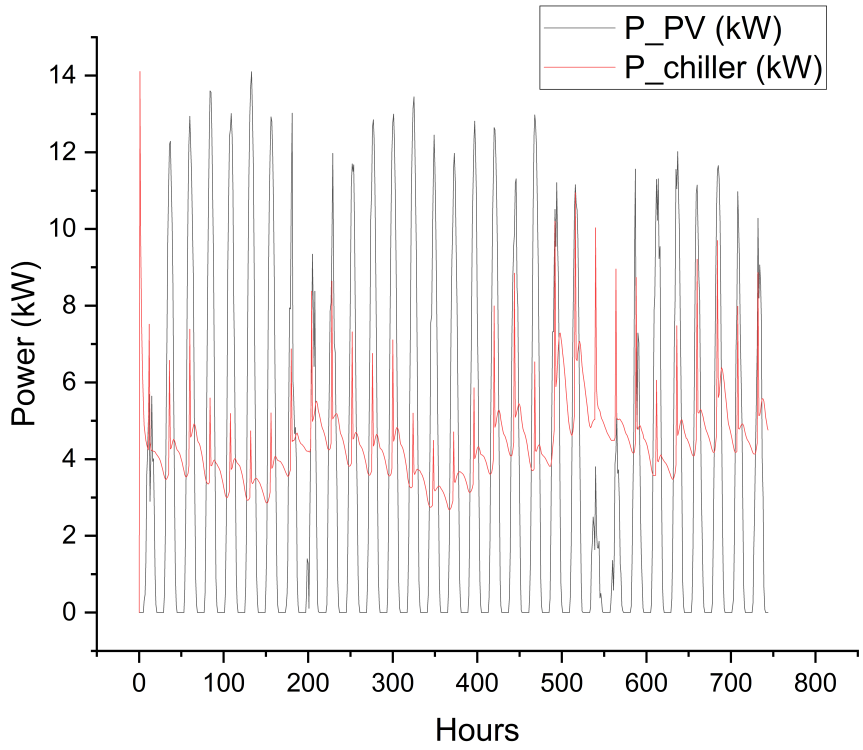

Figure 2.19: Comparison between $400m^2$ PV and chiller powers in July.

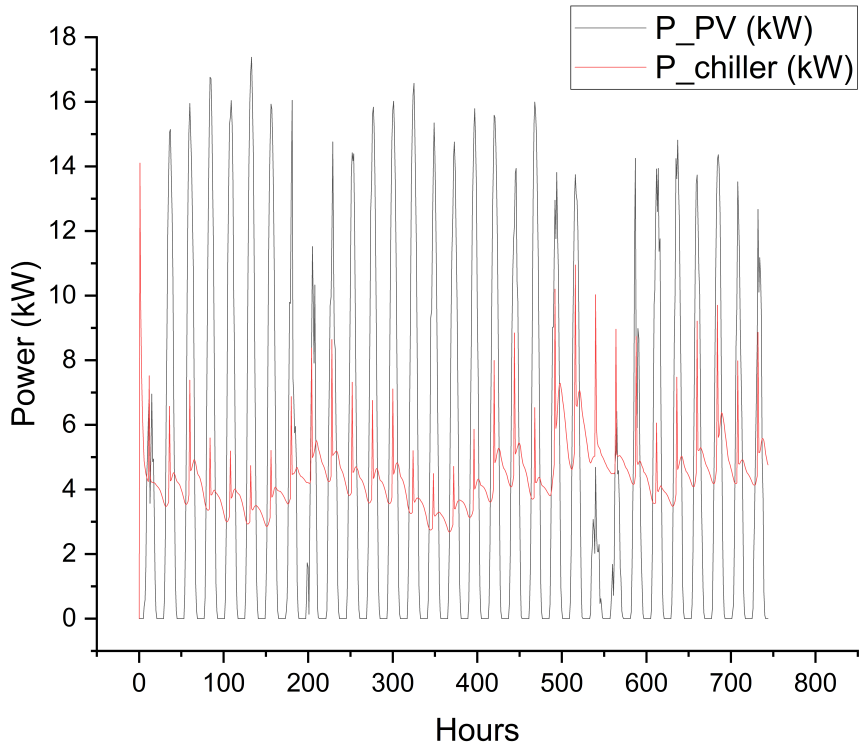

Figure 2.20: Comparison between $490m^2$ PV and chiller powers in July.

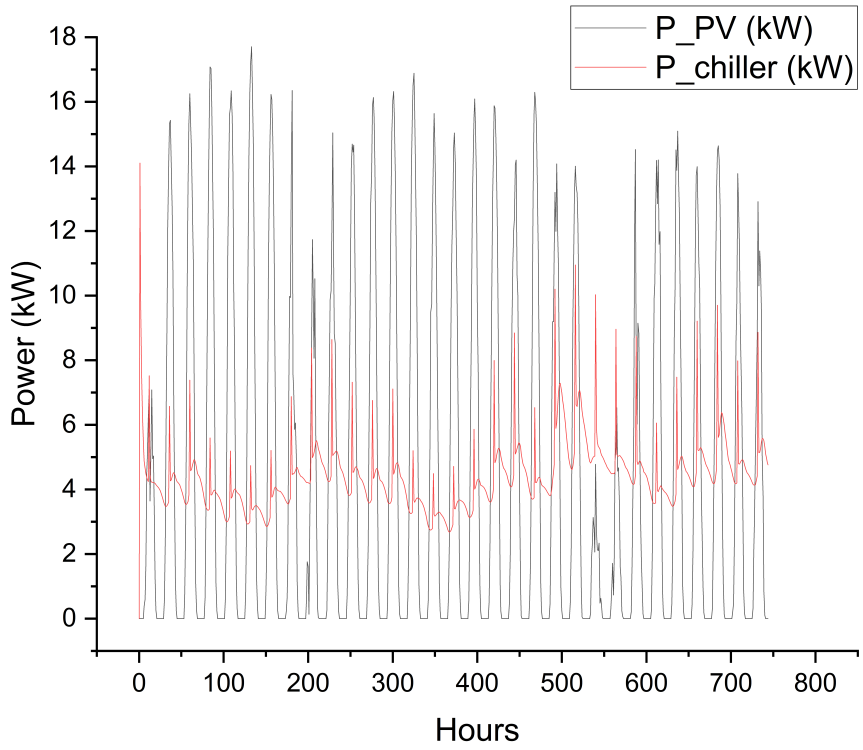

Figure 2.21: Comparison between $500m^2$ PV and chiller powers in July.

2.4.4 15th of January

PV areas of $1000m^2$ and $5000m^2$ were only tested for the 15th of January. The smallest value of deficit between the power of PV and chiller for a surface area of $5000m^2$ is 3.3 kW, as shown in figure 2.23. During a day in winter, only a few hours of PV electricity is generated, so a much larger area is needed to meet the chiller demand.

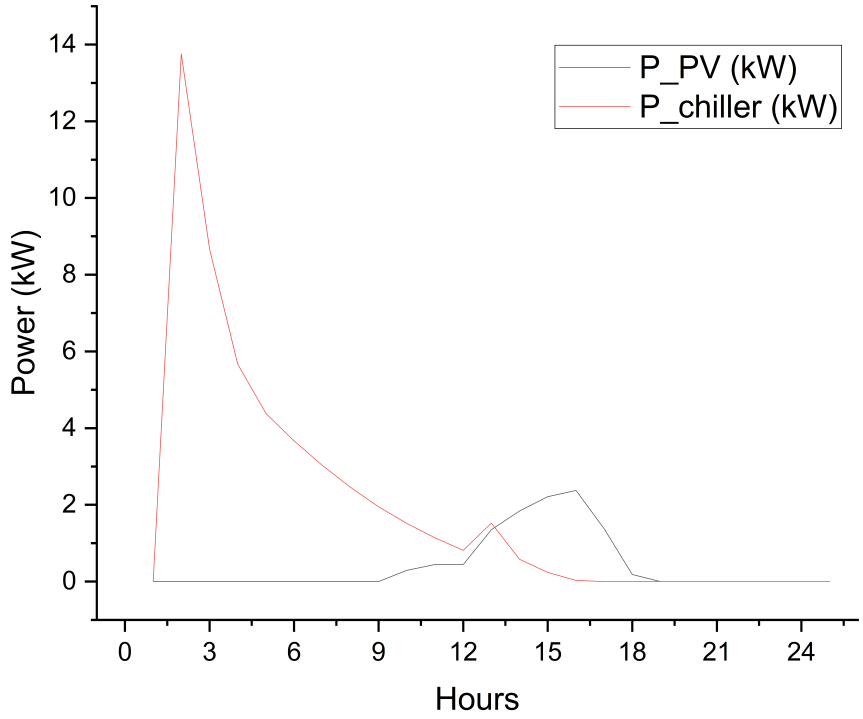

Figure 2.22: Comparison between $1000 m^2$ PV and chiller powers on 15th of January.

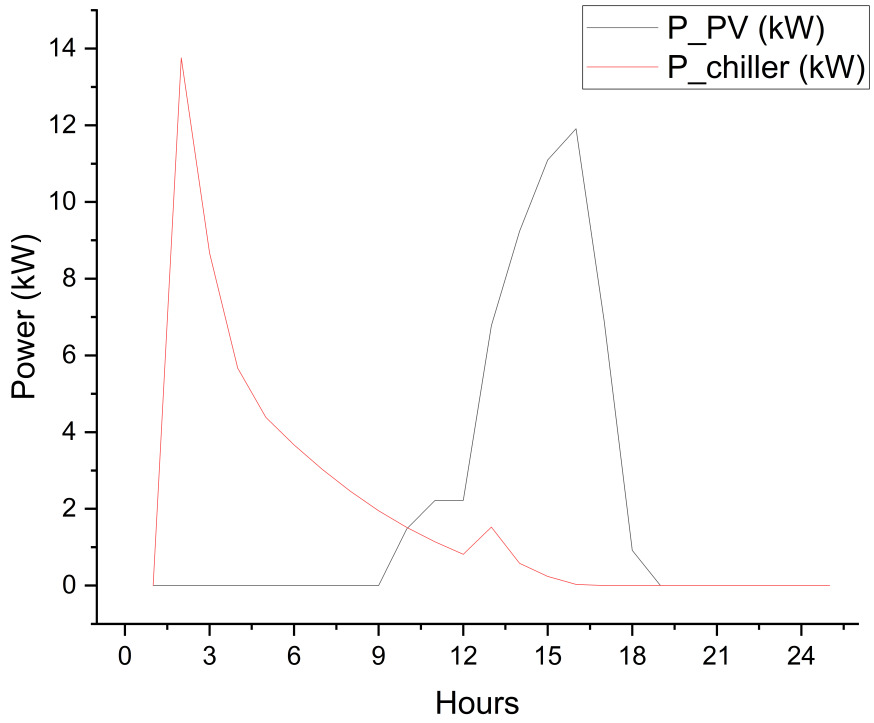

Figure 2.23: Comparison between $5000m^2$ PV and chiller powers on 15th of January.

2.4.5 15th of July

Both $480m^2$ and $500m^2$ of photovoltaic panels were checked on the 15th of July. Figure 2.25 shows that the minimal difference between the power of PV and chiller is 2.3 kW when applied to a PV surface area of $500m^2$.

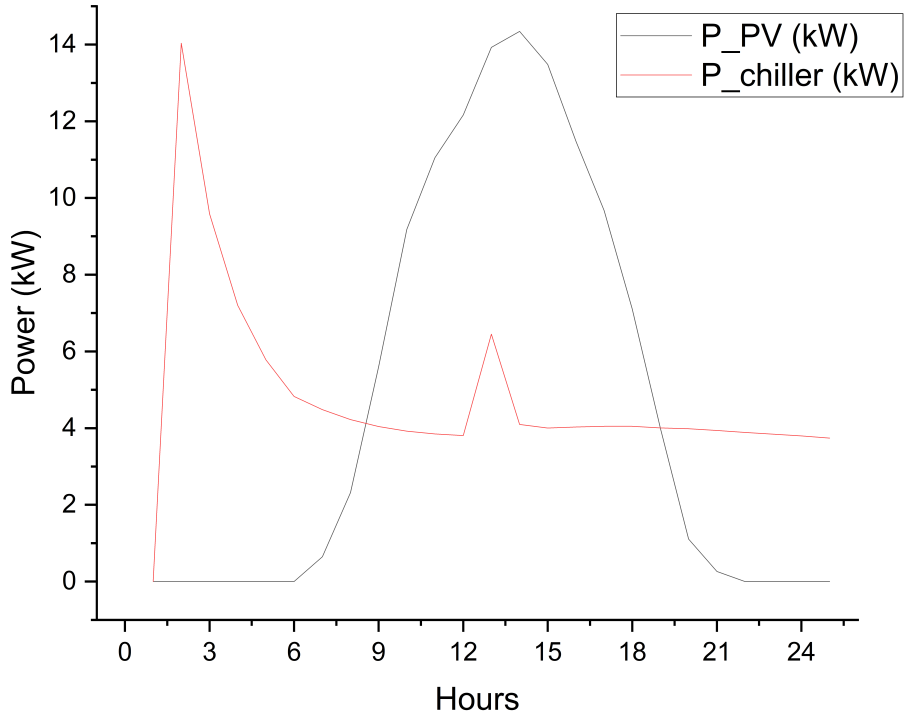

Figure 2.24: Comparison between $480m^2$ PV and chiller powers on 15th of July.

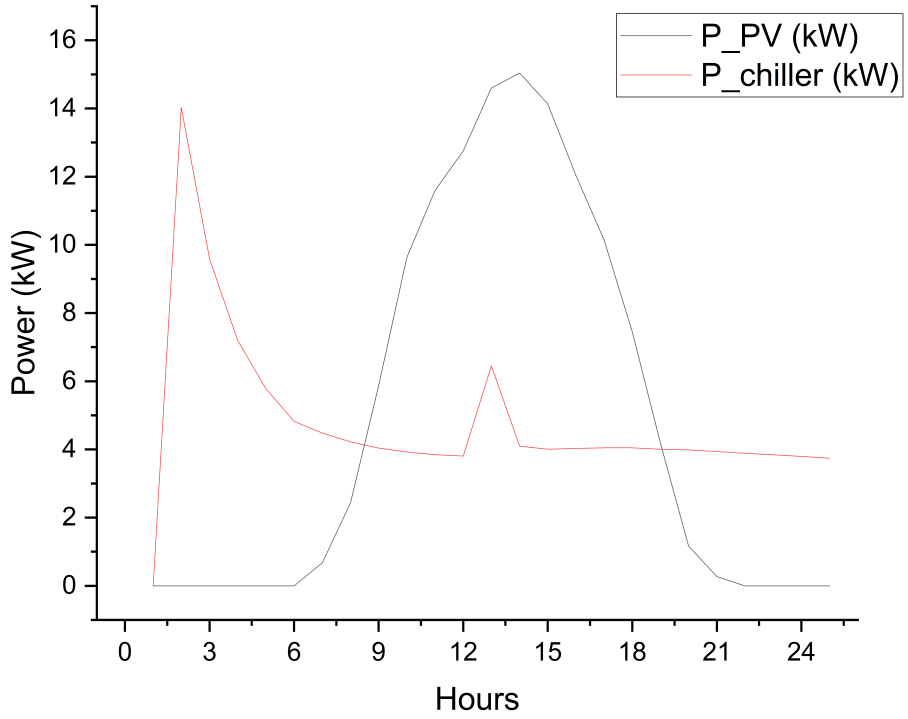

Figure 2.25: Comparison between $500m^2$ PV and chiller powers on 15th of July.

3
Results

Simulations were carried out to further understand from the energy point of view how changing the size of the PV modules would affect the total amount of electricity saved while using thermal energy storage. In order to better visualize and understand the seasonal fluctuations, four different PV modules and chiller were simulated on an hourly basis in 4 different months (January, April, July, and October). EXCEL was used to figure out how much electricity was saved by getting the electricity data from TRNSYS for the PV panels and chiller. Different TES capacities such as 10 kWh, 20 kWh, 50 kWh and 100 kWh were assumed, which all would initially be empty. All calculations were made assuming two different cases.

1. When $P_{PV} > P_{Chiller}$, PV was utilized to run the chiller and TES was used to store any remaining energy. In this situation, we are able to save as much as the sum of hourly electricity needed to run the chiller since that electricity is generated entirely by PV panels.

$$\Sigma P_{Chiller} = SavedElectricity$$

2. When $P_{PV} < P_{Chiller}$,

$$P_{PV} > 0, \Sigma P_{PV} = SavedElectricity$$

Chiller was powered entirely by energy drawn from TES. Here, as a result of using storage, we are able to save as much electricity as the total amount of

electricity released from our energy storage system.

Cold storage was cooled using the energy stored in the TES. Here, as a result of using storage, we are able to save as much electricity as the total amount of electricity released from our energy storage system.

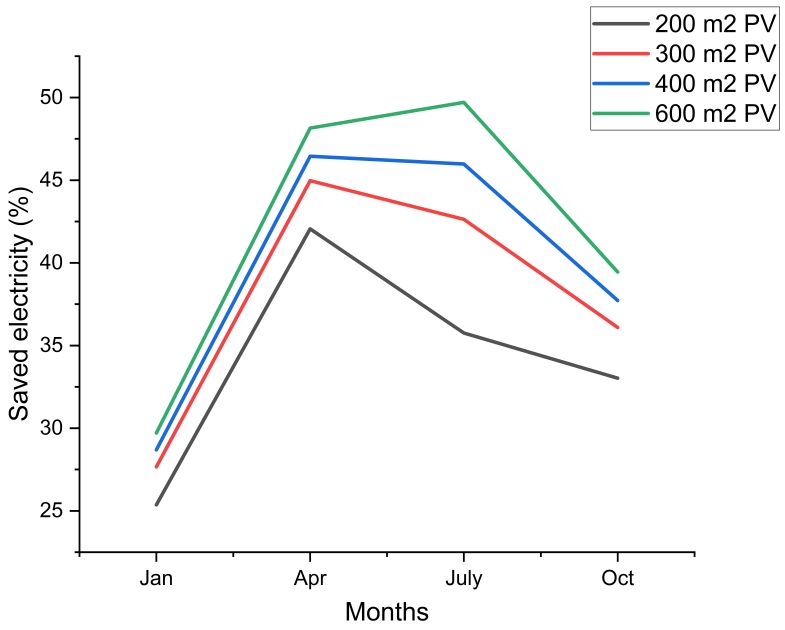

Figure 3.1: Saved electricity percentages using only PV.

Figure 3.1 shows the monthly percentages of energy saved by using only certain PV areas. The percentage rises from increasing the PV area from $200m^2$ to $600m^2$ are just 4% in January, 6% in April, 15% in July, and 5% in October. The low percentages for the month of July are due to the fact that the solar energy generated cannot meet the cooling demand. Only using a $600m^2$ PV area saves 50% of the electricity demand of the chiller.

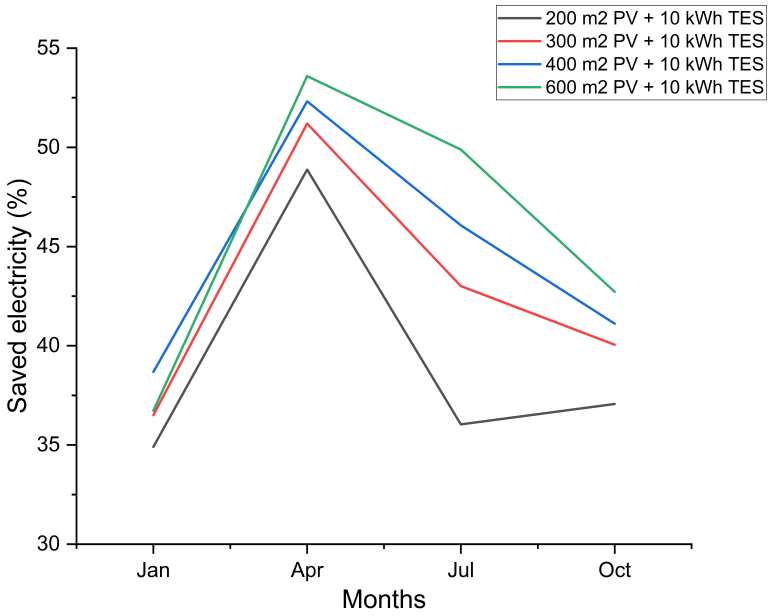

Figure 3.2: Saved electricity percentages using PV and 10 kWh TES.

Percentages of energy saved by using different PV areas with 10 kWh TES is shown above. The use of TES helps save more energy. It is obvious that using a larger PV area such as $600m^2$ for January does not result in much energy savings. For July, the difference between the use of $200m^2$ and $600m^2$ is the largest at around 14%.

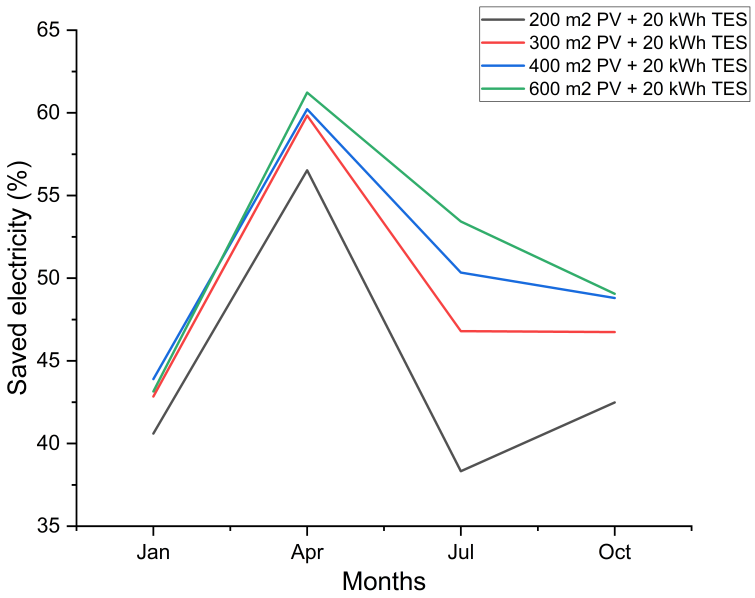

Figure 3.3: Saved electricity percentages using PV and 20 kWh TES.

Different PV areas with 20 kWh TES result in varying percentages of energy savings, as indicated above. From this graph, it can be concluded that the use of $300m^2$ and $600m^2$ of PV area for January will provide the same savings if 20 kWh TES is used. Also, increasing the PV area from $400m^2$ to $600m^2$ in October will not change much in percentage terms.

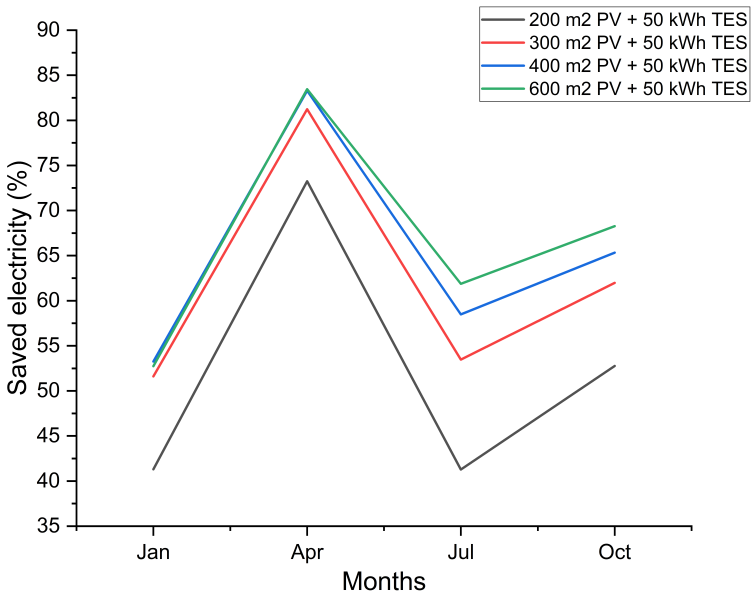

Figure 3.4: Saved electricity percentages using PV and 50 kWh TES.

Figure 3.4 illustrates the percentage of energy savings obtained by various PV areas using 50 kWh TES. There is no advantage to increasing the area beyond the first $300m^2$ of PV used with 50 kWh of TES throughout January and April. Both a $400m^2$ and a $600m^2$ PV area will provide savings of up to 83% in April, but only the smaller one will be cost-effective.

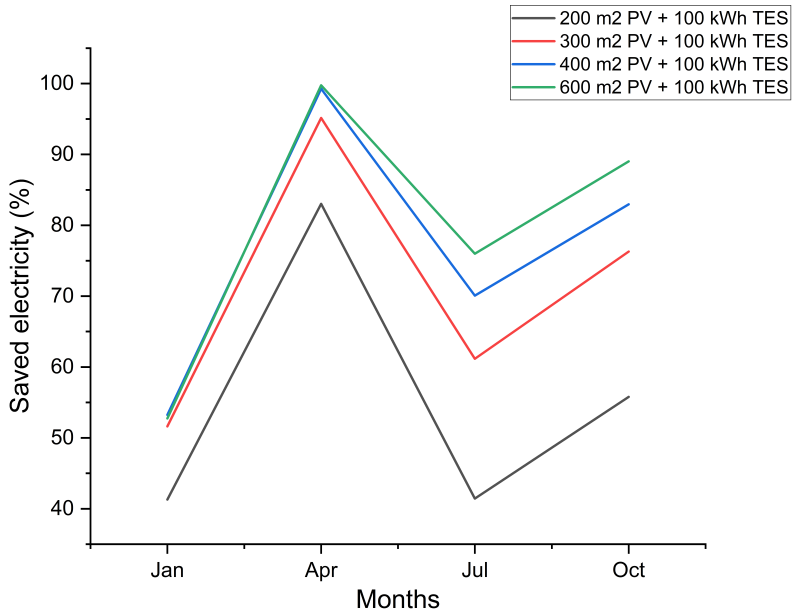

Figure 3.5: Saved electricity percentages using PV and 100 kWh TES.

The above graph demonstrates the percentage of energy that may be saved by installing 100 kWh TES in a variety of PV systems. It is shown that the energy percentage does not rise above a particular limit size of the TES for a given PV size.

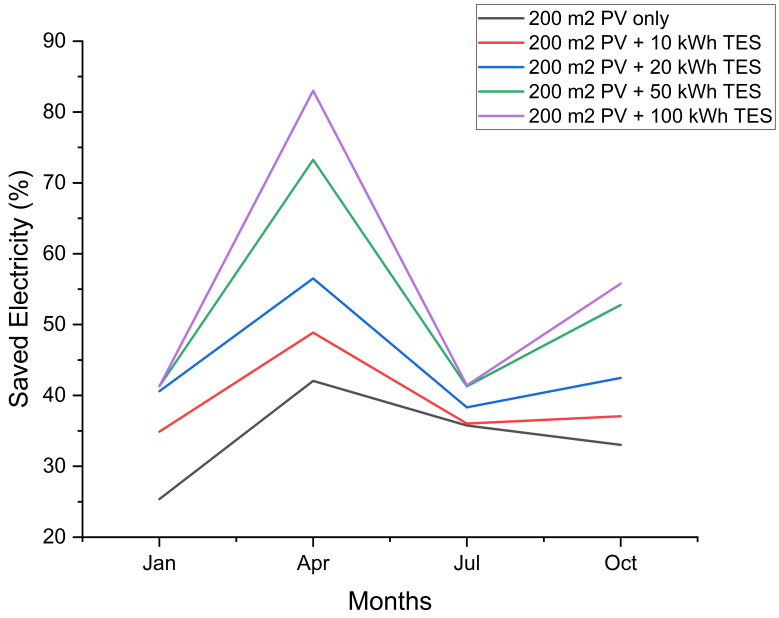

Figure 3.6: Saved electricity percentages using a different capacity of TES with $200 m^2$ PV.

The graph above shows that the proportion of energy saved improves when the size of the TES grows while the PV areas remain the same. Yet, even with a 100 kWh TES installed, efficiency does not improve in January. The ratio of saved energy to demand does not change much with increasing storage capacity in July, because even with TES PV area is not able to cover chiller demand.

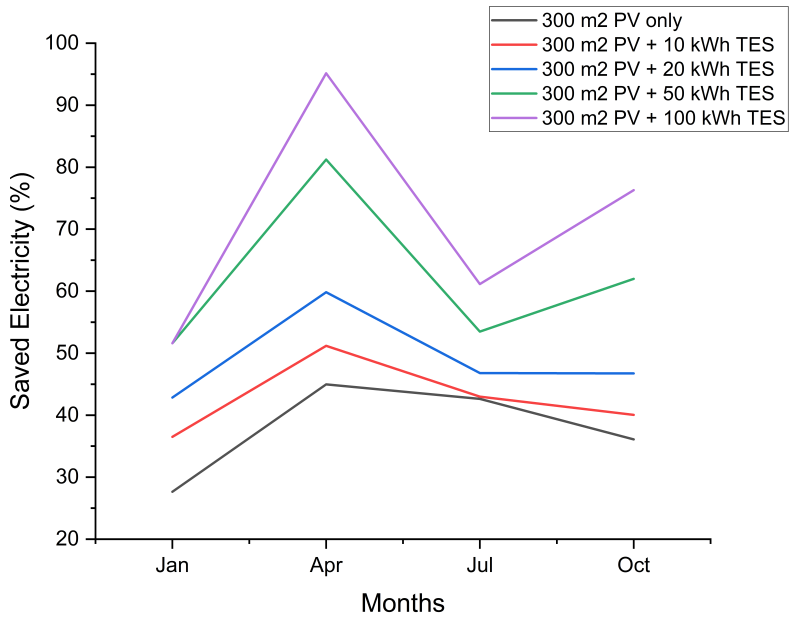

Figure 3.7: Saved electricity percentages using a different capacity of TES with $300m^2$ PV.

Figure 3.7 shows that in January up to 50% of energy can be saved and it would not be economically viable to use more than 50 kWh TES because the percentage would remain the same. In July, up to 61% of energy can be saved by using larger size TES, while smaller sizes will not affect much and the percentage of energy savings from only PV and 10 kWh of storage with PV will be the same 43%.

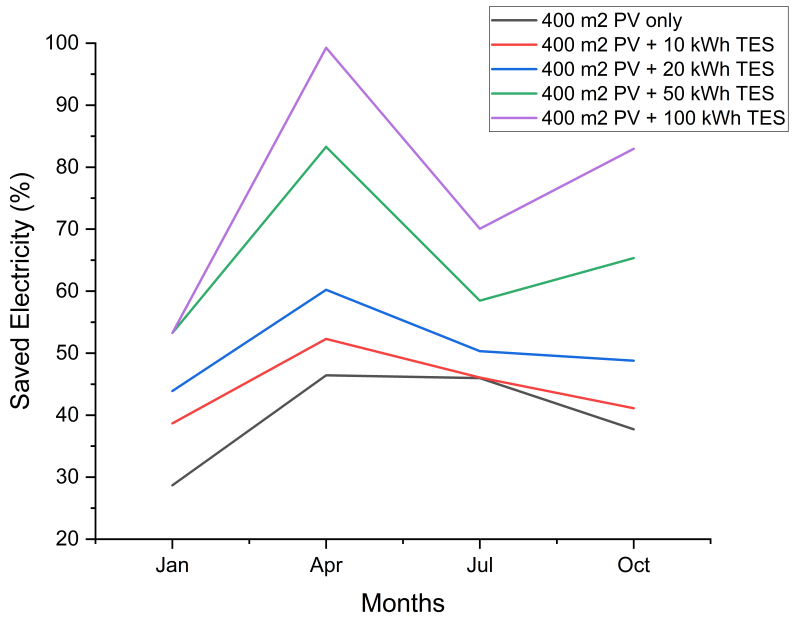

Figure 3.8: Saved electricity percentages using a different capacity of TES with $400m^2$ PV.

From figure 3.8, it is clear that the ratio of savings to demanding in July using a 100 kWh TES can be about 70%, whereas without TES it is 46%.

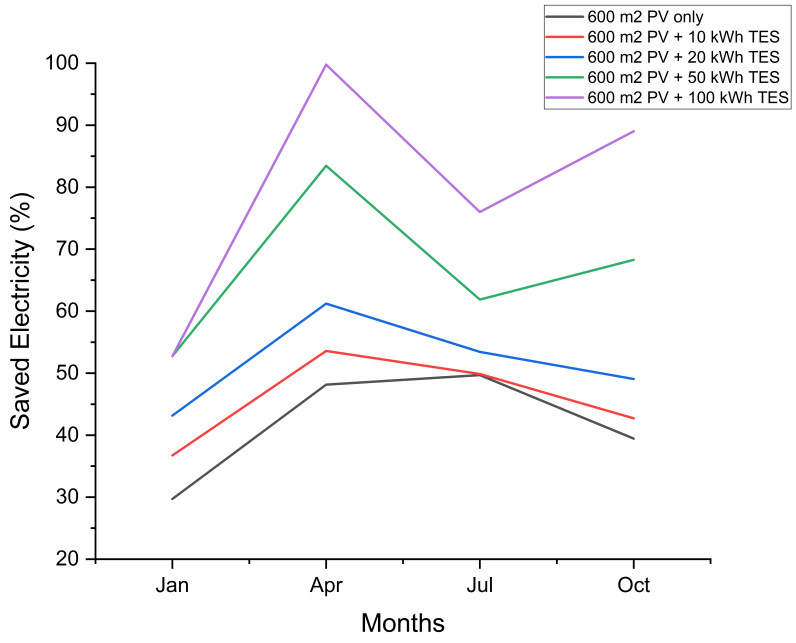

Figure 3.9: Saved electricity percentages using a different capacity of TES with $600m^2$ PV.

As seen also in this graph (figure 3.9), increasing the size of both TES and PV fields increases the efficiency of the system. In April, energy can be saved entirely with solar panels and storage.

3.1 PV area of $200m^2$

As it is mentioned before, energy savings in July were more than usual (528.69 kWh in total) because of the abundance of sunshine and the fact that our chiller draws most of its electricity (1170.78 kWh) from our photovoltaic system, that is why discharged energy (9.28 kWh) from 10 kWh TES is quite lower. Both PV and 10 kWh TES are used to power the chiller in the spring and fall; in April and October, the primary source of energy is PV, providing 475.13 and 490.1 kilowatt-hours, respectively, while the total quantity of electricity discharged is 77.04 and 60 kilowatt-hours. But, in January the chiller does not require a lot of energy due to the cold, so we don't use as much of either the PV panels or the TES; the chiller uses 25.47 kWh and 9.63 kWh of electricity from the PV and 10 kWh TES, accordingly.

The following figures illustrate seasonal changes in TES's electrical charging and discharging activity. As it is mentioned earlier, the quantity of charging and discharging power throughout the spring and autumn seasons is most noticeable since both PV and TES are operating during these times. As there is less demand for the TES during January, the TES is kept near to full charge throughout those months. In July, however, the chart patterns stay charged even at night since the energy from TES is not enough to power the chiller.

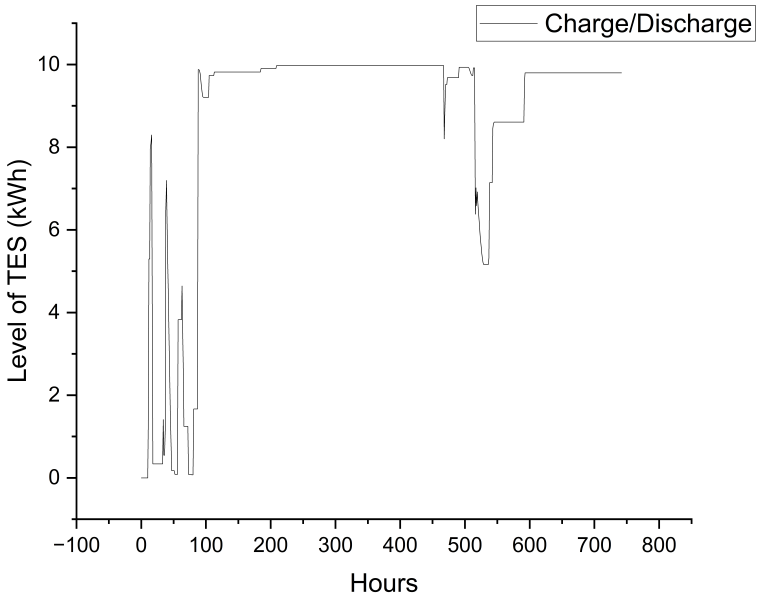

Figure 3.10: Level of TES with $200m^2$ PV in January.

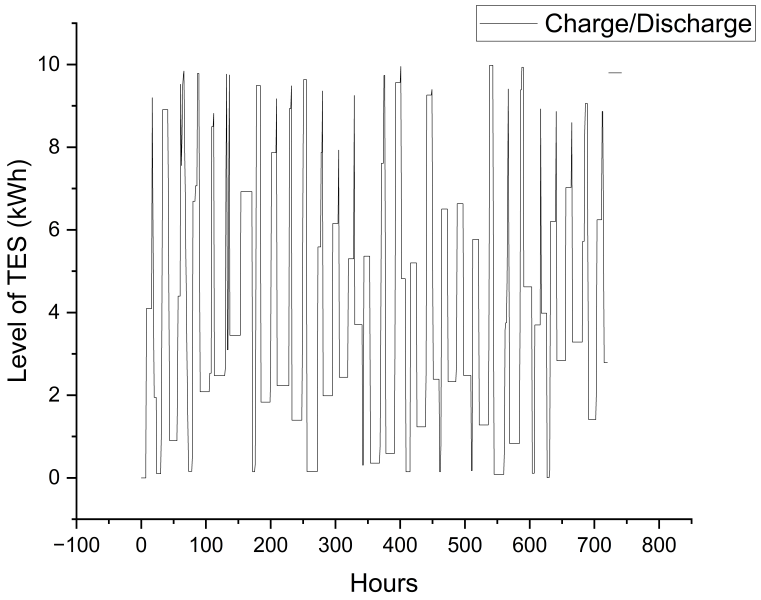

Figure 3.11: Level of TES with $200m^2$ PV in April.

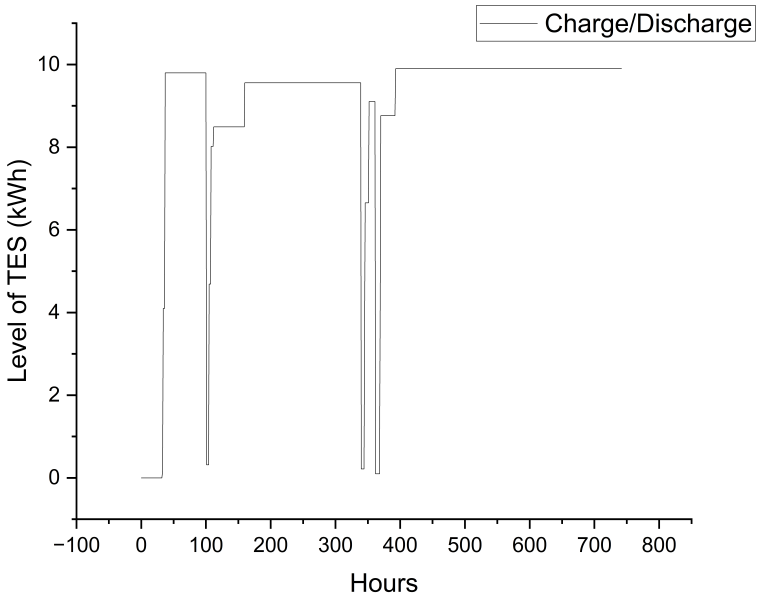

Figure 3.12: Level of TES with $200m^2$ PV in July.

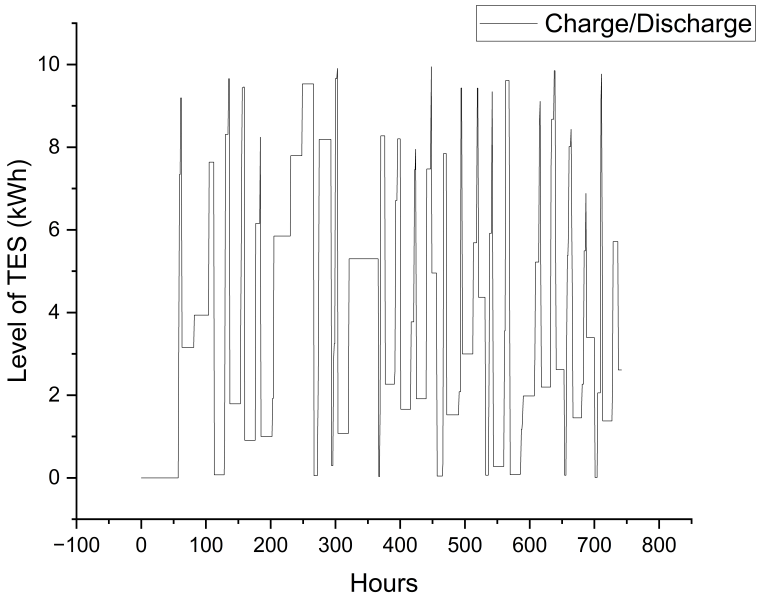

Figure 3.13: Level of TES with $200m^2$ PV in October.

3.2 PV area of $300m^2$

Calculations show that the amount of energy discharged (8.9 kWh) from the capacity of 10 kWh TES is lowest in January, but we still manage to operate the chiller (27.78 kWh) almost on PV-generated power. The quantity of electricity used to power the chiller came from PV rise in proportion to the area of PV, but less electricity is discharged by the TES as a result. This means that in April and October, respectively, 507.94 kWh and 535.46 kWh of electricity is fed into the chiller from the photovoltaic panels, while 70.55 kWh and 58.85 kWh are discharged from the thermal energy storage system. Chiller is powered with 1395.9 kWh of electricity from PV and 12.39 kWh from TES during July.

The following graphs are almost similar to the figures above since the underlying concepts are the same. Depending on the weather report there may be a few days in July when TES discharges electricity. For the majority of the summer, the storage may be charged since the TES is not producing enough electricity to run the chiller.

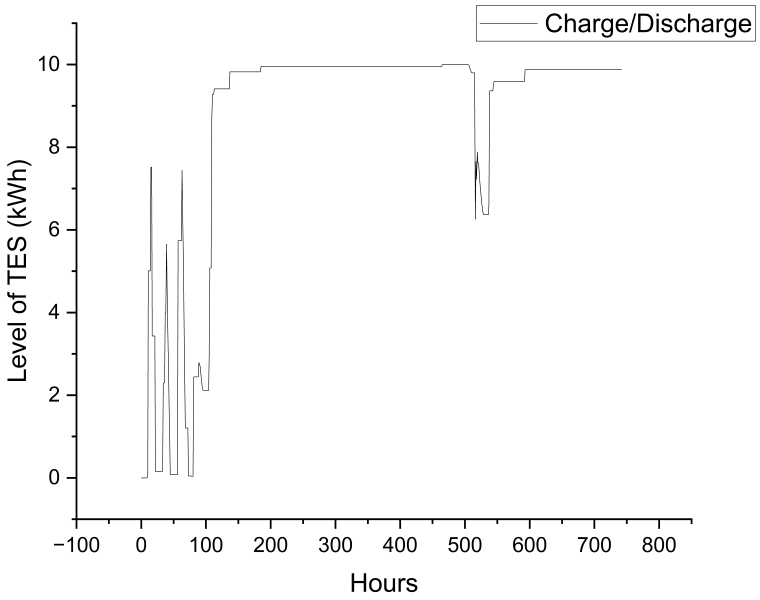

Figure 3.14: Level of TES with $300m^2$ PV in January.

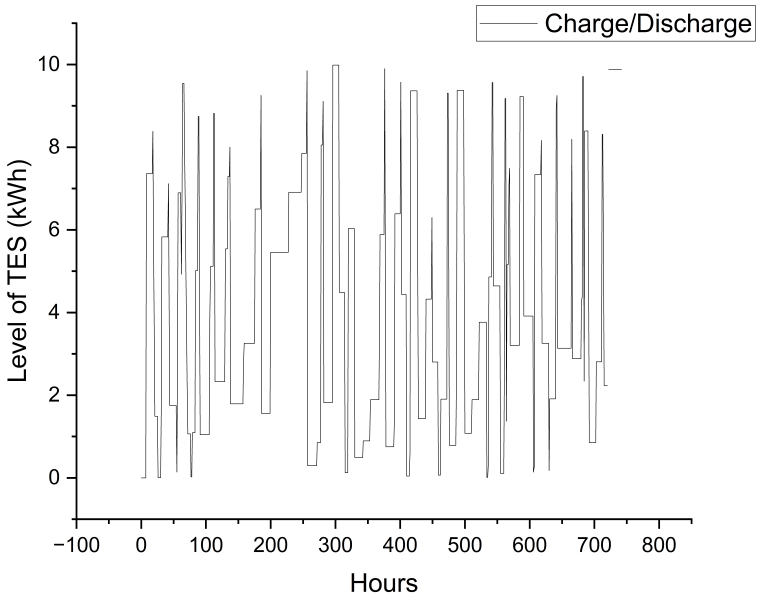

Figure 3.15: Level of TES with $300m^2$ PV in April.

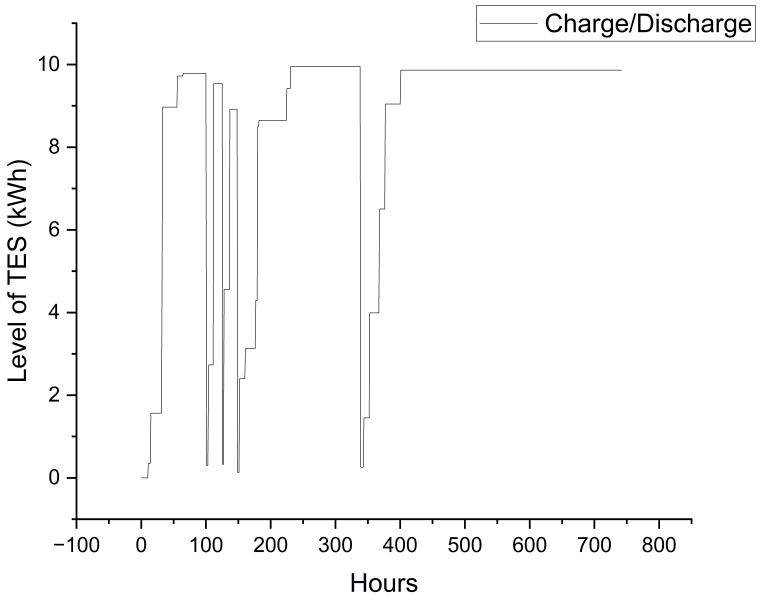

Figure 3.16: Level of TES with $300m^2$ PV in July.

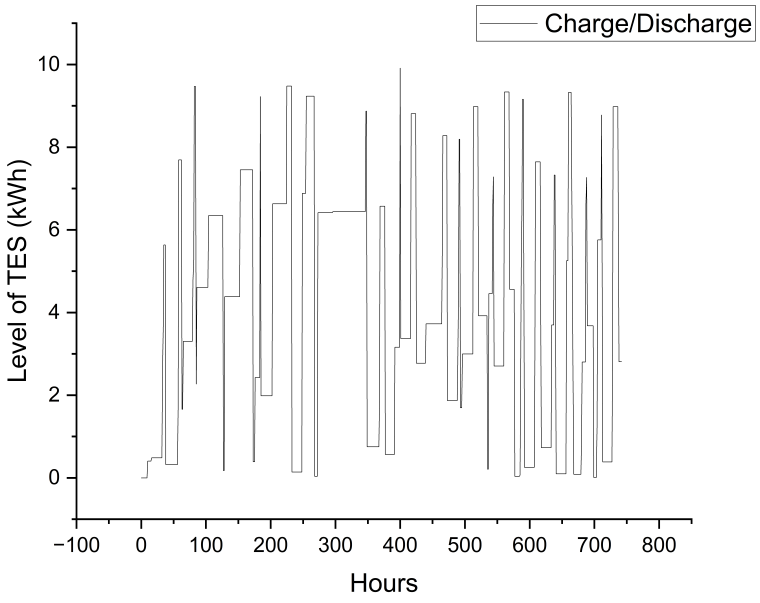

Figure 3.17: Level of TES with $300m^2$ PV in October.

3.3 PV area of $400m^2$

After installing a $400m^2$ area of PV panels, power supplied by the PV to the chiller rises while power supplied by the TES falls. Hence, the combined amount of electricity saved in April and October is 591 kWh and 610.06 kWh, respectively. In warmer seasons like July, when the chiller draws more electricity, electricity saved from PV is a grand total of 1505.3 kWh. In January, the chiller's energy use is minimal and the total saved energy is 38.9 kWh.

The following graphs show the level of a 10 kWh TES when energy is loaded and unloaded.

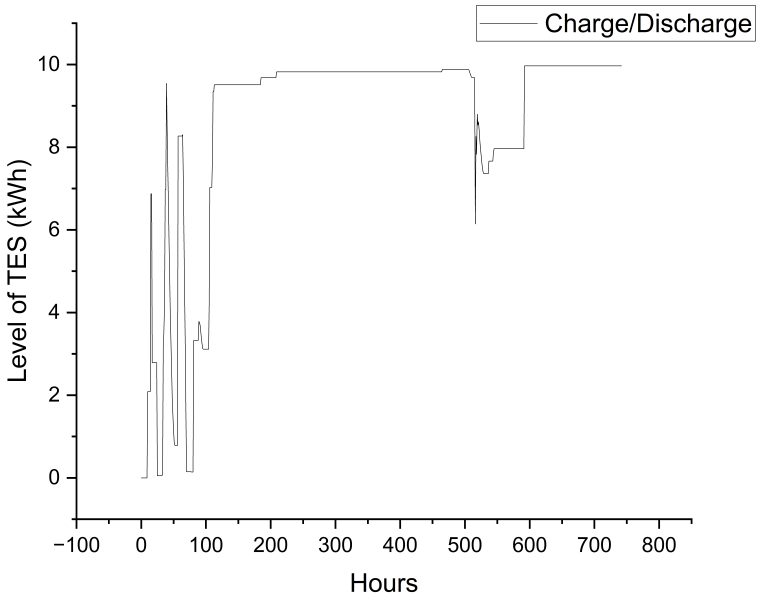

Figure 3.18: Level of TES with $400m^2$ PV in January.

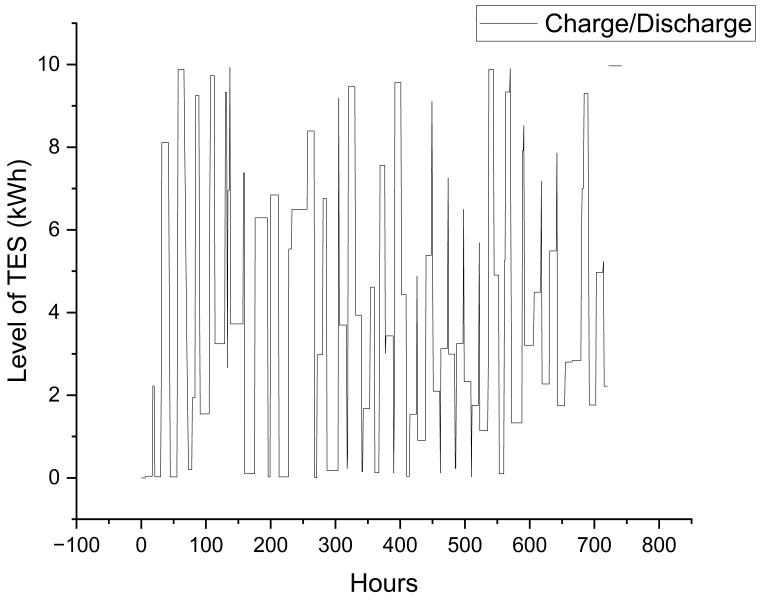

Figure 3.19: Level of TES with $400m^2$ PV in April.

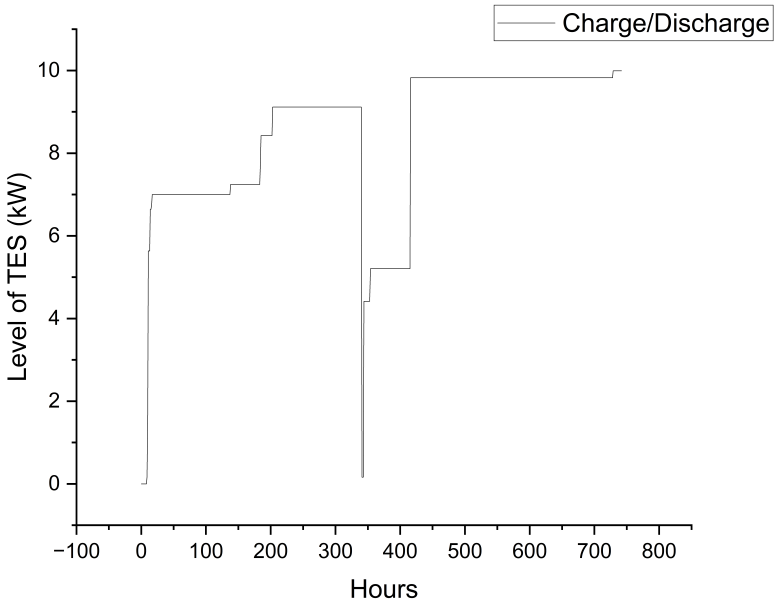

Figure 3.20: Level of TES with $400m^2$ PV in July.

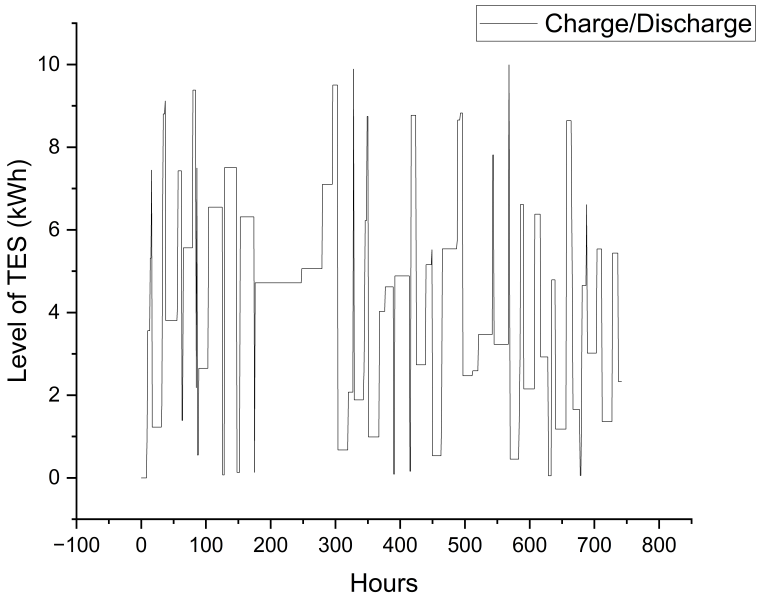

Figure 3.21: Level of TES with $400m^2$ PV in October.

3.4 PV area of $600m^2$

A similar pattern is seen with a PV area of 600 square meters. In January and July, 29.85 kWh and 1627.34 kWh of power are used by the chiller from PV, whereas 7.04 kWh and 6.17 kWh are used by the chiller from the TES, respectively. The chiller's energy demands are lower in the winter and greater in the summer, creating a significant seasonal variation. In April and October, PV supplies 543.84 kWh and 585.28 kWh of power to the chiller, whereas TES discharges 61.61 kWh and 48.58 kWh of electricity to the chiller, respectively.

The graph below depicts the 10 kWh TES charged electricity amount when PV power is larger than the power required by the chiller, and the discharged amount when PV is less.

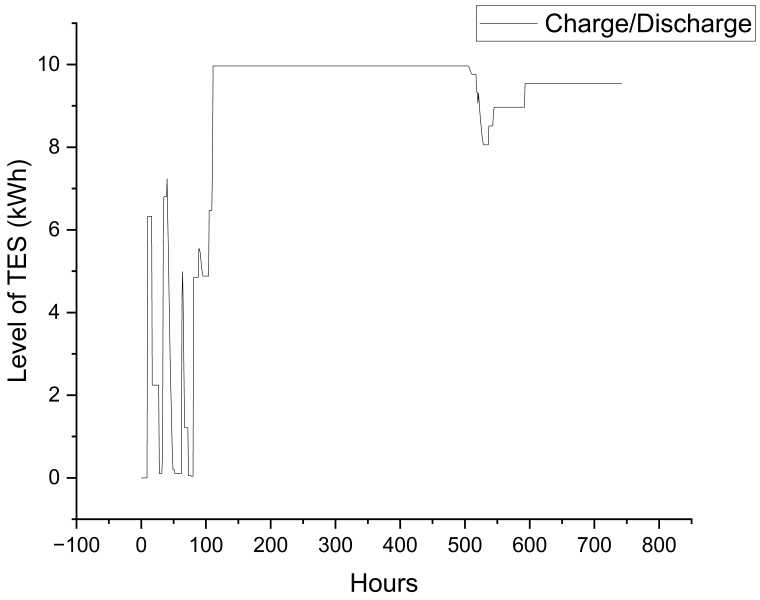

Figure 3.22: Level of TES with $600m^2$ PV in January.

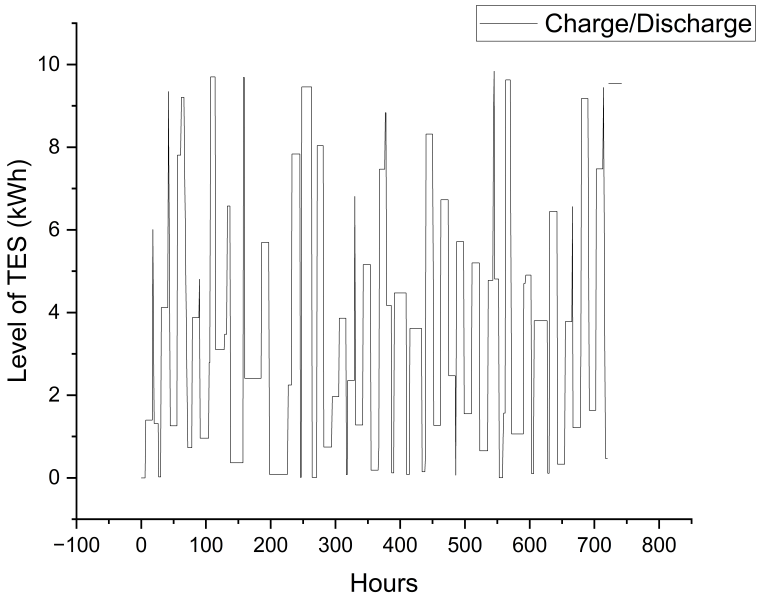

Figure 3.23: Level of TES with $600m^2$ PV in April.

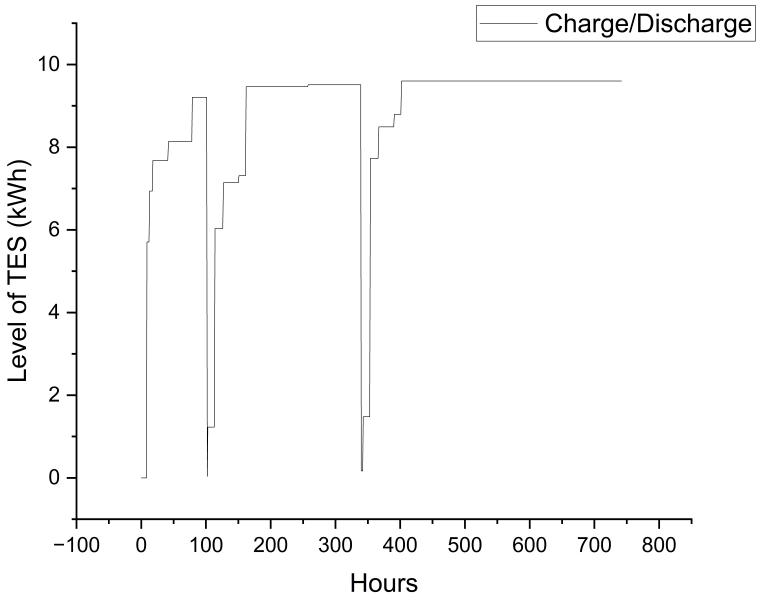

Figure 3.24: Level of TES with $600m^2$ PV in July.

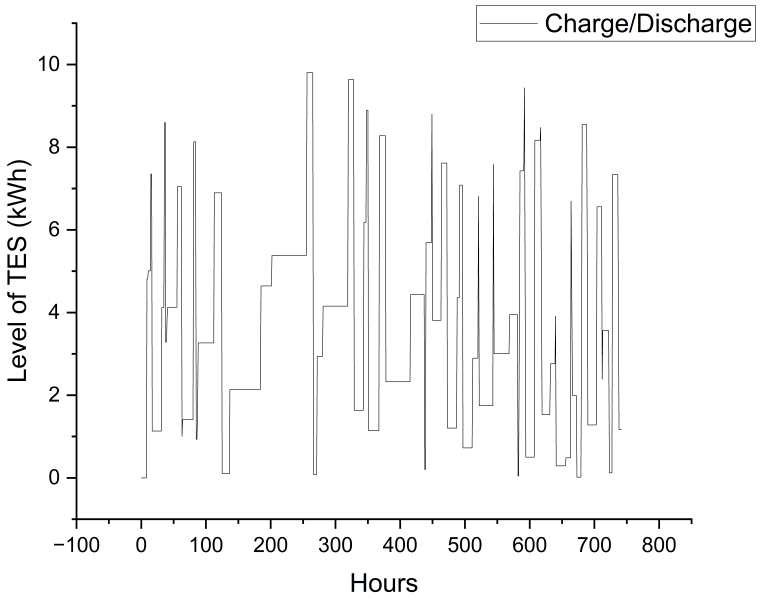

Figure 3.25: Level of TES with $600m^2$ PV in October.

3.5 Annual analysis

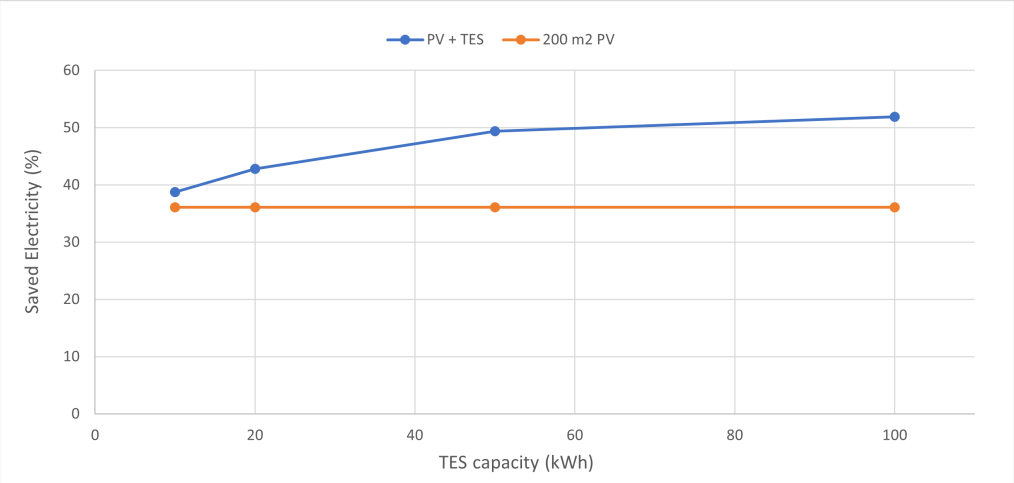

Figure 3.26: Annual saved energy (%) with $200m^2$ PV and different TES capacities.

Without thermal energy storage, the system saves about 36% of energy with $200m^2$ PV alone. When the storage size is increased from 10 kWh to 20 kWh, the percentage of energy saved rises by 10%, while from 20 kWh to 50 kWh there is an increase of 15%. However, when the storage capacity is doubled from 50 kWh to 100 kWh, there is a very small growth of about 5%. This means that for a PV area of $200m^2$ there is no need to increase the TES capacity after 50 kWh.

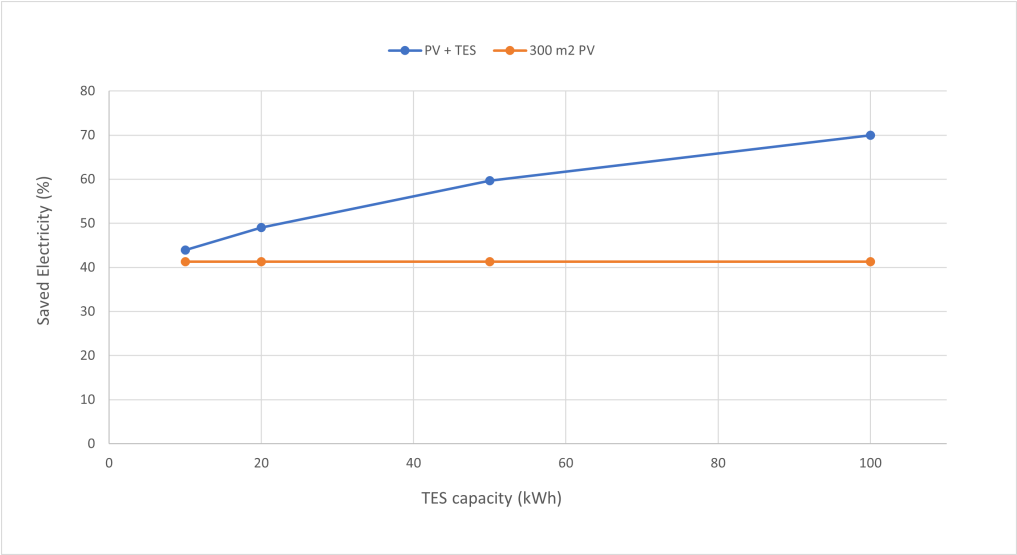

Figure 3.27: Annual saved energy (%) with $300m^2$ PV and different TES capacities.

Around 41.3% of the system's energy demand can be met by $300m^2$ PV alone, without having thermal energy storage. The proportion of energy saved grows by 12% when going from 10 kWh to 20 kWh of storage, and by 22% when going from 20 kWh to 50 kWh of TES. A similar increase of about 17% is seen when rising from 50 kWh to 100 kWh of storage capacity.

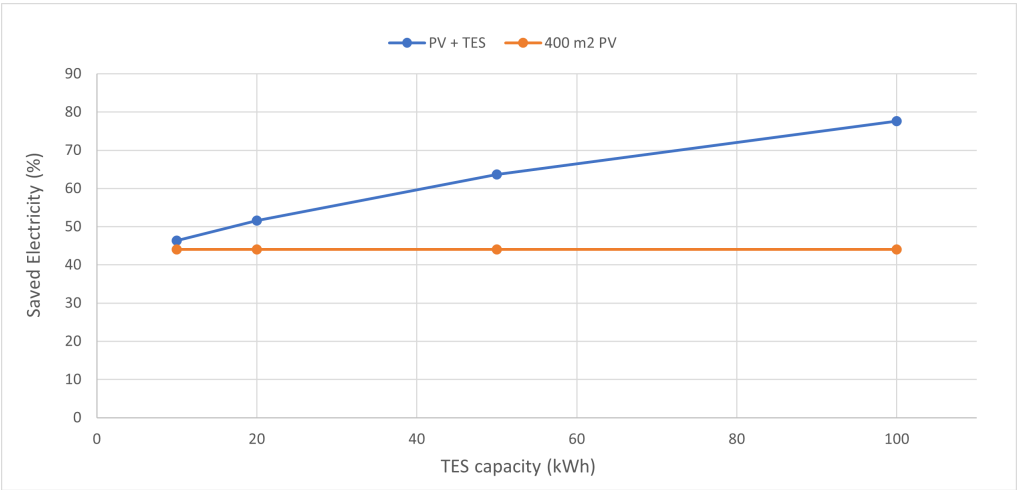

Figure 3.28: Annual saved energy (%) with $400m^2$ PV and different TES capacities.

Without TES, $400m^2$ PV alone can provide about 44% of the system's energy needs. Energy savings increase by 24% when the storage capacity goes from 20

kWh to 50 kWh and by 12% when the storage capacity rises from 50 kWh to 100 kWh. Similar to the $300m^2$ PV area, there is also an increase of about 12% when going from 10 kWh to 20 kWh storage capacity.

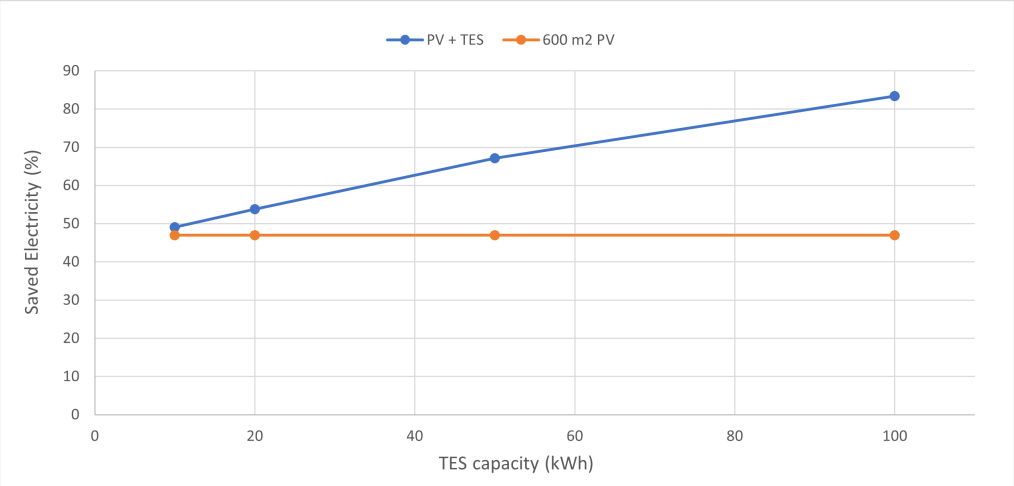

Figure 3.29: Annual saved energy (%) with $600m^2$ PV and different TES capacities.

$600m^2$ of PV without TES can provide 47% of the system's energy. Energy savings rise 9.5% from 10 kWh to 20 kWh and 25% from 20 kWh to 50 kWh TES. Rising from 50 kWh to 100 kWh, saved to demand energy ratio improves 24%. Expanding the PV area and staying with smaller TES capacities (10 kWh) does not make any difference in energy savings compared to PV savings alone.

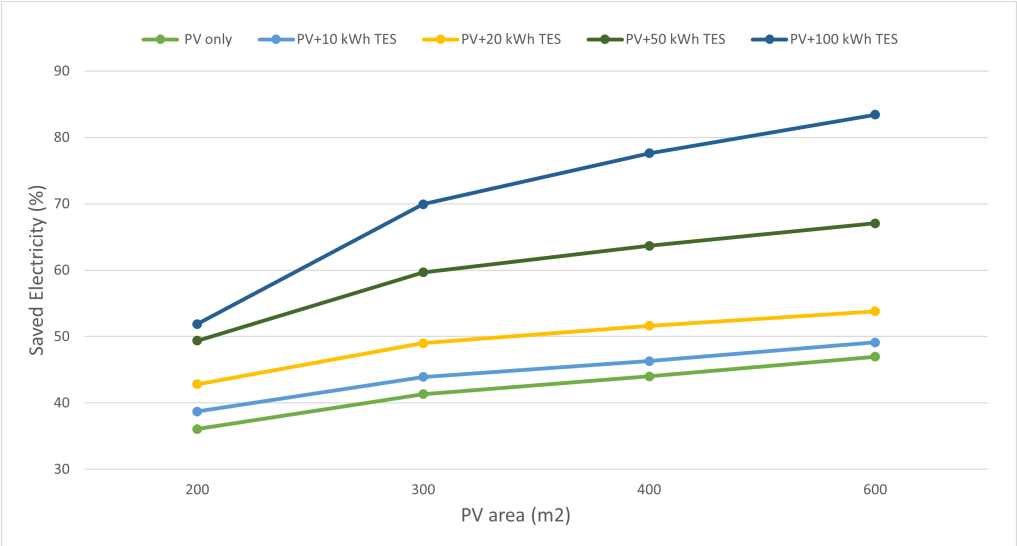

Figure 3.30: Annual saved energy (%) with different PV and TES.

Figure 3.30 shows that the efficiency of PV systems grows sharply from $200m^2$ to $300m^2$, but the curve flattens out between $300m^2$ and $600m^2$. While expanding PV from 200 to 300 square meters, the PV+100 kWh TES line's energy savings improve by 37%, but they only grow by 16% when expanding from 300 to 600 square meters. Using TES of small size (10 kWh, 20 kWh) over all PV areas increases energy savings by just a small margin. As can be seen from the graph, increasing the TES size and decreasing the PV size have a positive impact in terms of both economics and energy.

4
Conclusion

The purpose of this thesis was to investigate and assess the performance of a PV-powered cold chain container that had an integrated TES in Venice, Italy. The goals of this study were accomplished by the use of TRNSYS software for the modelling and simulation of a solar-powered refrigerated container system. Keeping the $5000m^3$ cold storage container by opening the door for only one hour a day was made possible with the use of TRNBuild, a visual interface of TRNSYS. Further particular details, such as building material, heat gains, timetables, and meteorological data, were included in the simulation tools of PV, the chiller, and the container. The mass flow rate required by the chiller to meet the cooling load of the container (average peak 50.7 kW in August) was determined by fixing the inlet (4) and outlet (2) temperatures of the chiller. Then, we compared the annual, monthly, and daily electricity generated by PV in different areas and the power needed by the chiller by linking the weather and location data with PV and inserting the necessary parameters. Assuming 10 kWh, 20 kWh, 50 kWh and 100 kWh of thermal energy storage, we determined how much electricity could be saved by installing PV panels with $200m^2$, $300m^2$, $400m^2$ and $600m^2$ surface areas.

- For a $200m^2$ PV area, we are able to save 25.47 kWh of electricity in January, 475.13 kWh in April, 1170.78 kWh in July and 490.1 kWh in October without TES. As the chiller uses more power in the summer and the PV panels cannot meet chiller demand even at night. So even installing 100 kWh TES capacities

can rise saved electricity percentage by up to 42%, which is quite similar to saving with 50 kWh TES in July. In January saved energy percentage is 41% with both 50 kW and 100 kWh TES, this means beyond the 50 kWh size of TES, efficiency does not increase and installing larger TES can be economically expensive.

- Electricity savings of 27.78 kWh in January, 507.94 kWh in April, 1395.9 kWh in July, and 535.46 kWh in October were achieved with only a PV area of $300m^2$. More electricity is obtained from TES in the fall and spring than at any other time of year, even though the PV panel covers the chiller's electrical needs in those seasons. Increasing TES capacities up to 100 kWh, rise also saved energy percentage to around 51% in January and 62% in July.

- In January, we are able to save 28.82 kWh, in April 524.73 kWh, in July 1505.3 kWh and in October 55.75 kWh, all using only a PV area that was $400m^2$ in size. While TES capacity rises, saved energy percentages also increase but for July, putting small size TES (10 kWh) saves the same percentage of energy even with only PV area.

- For a $600m^2$ PV area, we are able to save electricity of 29.85 kWh in January, 543.84 kWh in April, 1627.34 kWh in July and 58528 kWh in October. With higher TES installed, more electricity can be saved and less drawn from the grid.

- As the chiller uses less power and TES is kept almost fully charged throughout the winter, the total amount of energy saved is then at its lowest even with different TES capacities.

- In summer months, increasing both PV and TES size improves the efficiency of the system, but for smaller PV areas even installing high-capacity of TES does not make that much difference.

- As the chiller needs more energy to operate in summer, and small PV areas are not able to cover fully this amount even with TES, the level of TES almost remains charged even at night.

- On an annual basis, both the energy and cost savings may be further improved by increasing the TES size and lowering the PV size.

- This work was the first step to build a robust model to simulate the system behavior. It can be now applied to different location to show the real benefit of the application of TES technology.

References

[1] [Online]. Available: https://www.iea.org/fuels-and-technologies/cooling

[2] B. Diaconu, "Energy analysis of a solar-assisted ejector cycle air conditioning system with low temperature thermal energy storage," *Renewable Energy*, vol. 37, p. 266–276, 01 2012.

[3] [Online]. Available: https://www.ipcc.ch/report/ar6/wg3/

[4] X. Wu, "High-efficiency polycrystalline cdte thin-film solar cells," *Solar Energy*, vol. 77, no. 6, pp. 803–814, 2004, thin Film PV. [Online]. Available: https://www.sciencedirect.com/science/article/pii/S0038092X04001434

[5] Y. Gao, J. Ji, Z. Guo, and P. Su, "Comparison of the solar PV cooling system and other cooling systems," *International Journal of Low-Carbon Technologies*, vol. 13, no. 4, pp. 353–363, 09 2018. [Online]. Available: https://doi.org/10.1093/ijlct/cty035

[6] Q. Al-Yasiri, M. Szabó, and M. Arıcı, "A review on solar-powered cooling and air-conditioning systems for building applications," *Energy Reports*, vol. 8, pp. 2888–2907, 2022. [Online]. Available: https://www.sciencedirect.com/science/article/pii/S2352484722001731

[7] T. Otanicar, R. Taylor, and P. Phelan, "Prospects for solar cooling – an economic and environmental assessment," *Solar Energy*, vol. 86, p. 1287–1299, 05 2012.

[8] M. Mokhtar, M. T. Ali, S. Bräuniger, A. Afshari, S. Sgouridis, P. Armstrong, and M. Chiesa, "Systematic comprehensive techno-economic assessment of solar cooling technologies using location-specific climate data," *Applied Energy*, vol. 87, no. 12, pp. 3766–3778, 2010. [Online]. Available: https://www.sciencedirect.com/science/article/pii/S0306261910002539

[9] T. C. Roumpedakis, S. Vasta, A. Sapienza, G. Kallis, S. Karellas, U. Wittstadt, M. Tanne, N. Harborth, and U. Sonnenfeld, "Performance results of a solar adsorption cooling and heating unit," *Energies*, vol. 13, no. 7, 2020. [Online]. Available: https://www.mdpi.com/1996-1073/13/7/1630

[10] Y. Li and R. Wang, *Photovoltaic-powered solar cooling systems*, 12 2016, pp. 227–250.

[11] M. Shanmugam, N. Mangalasamy, and R. Manirathinam, "Design and analysis of solar vapour compression refrigeration system– a review," 2016.

[12] I. Sarbu and C. Sebarchievici, "A comprehensive review of thermal energy storage," *Sustainability (Switzerland)*, vol. 10, 01 2018.

[13] [Online]. Available: https://www.britannica.com/place/Venice

[14] [Online]. Available: https://population.un.org/wpp/

[15] [Online]. Available: https://mayorsofeurope.eu/top-stories/venice-to-establish-new-green-energy-resource-through-the-use-of-algae/

[16] [Online]. Available: https://statistica.regione.veneto.it/ENG/Pubblicazioni/RapportoStatistico2019/capitolo-4.jsp

[17] [Online]. Available: https://www.mise.gov.it/images/stories/documenti/SEN_EN_marzo2013.pdf

[18] Y. Xu and M. Li, "Impact of instantaneous solar irradiance on refrigeration characteristics of household pcm storage air conditioning directly driven by distributed photovoltaic energy," *Energy Science Engineering*, vol. 10, 01 2022.

[19] M. Asim, J. Dewsbury, and S. Kanan, "Trnsys simulation of a solar cooling system for the hot climate of pakistan," *Energy Procedia*, vol. 91, pp. 702–706, 2016, proceedings of the 4th International Conference on Solar Heating and Cooling for Buildings and Industry (SHC 2015). [Online]. Available: https://www.sciencedirect.com/science/article/pii/S1876610216303319

[20] [Online]. Available: https : / / theengineeringmindset . com / cooling-load-calculation-cold-room/

[21] [Online]. Available: https://www.solarchoice.net.au/products/panels/size/